Quinoline- and coumarin-based ligands and their rhenium(I) tricarbonyl complexes: synthesis, spectral characterization and antiproliferative activity on T-cell lymphoma

Martina Piškor[a], Ivan Ćorić[b], Berislav Perić[c], Katarina Mišković Špoljarić[b], Srećko I. Kirin[c],
Ljubica Glavaš-Obrovac[b*] and Silvana Raić-Malić[a*]

[a] *Department of Organic Chemistry, University of Zagreb, Faculty of Chemical Engineering and Technology, Marulićev trg 19, 10000 Zagreb, Croatia*
[b]*Department of Medicinal Chemistry, Josip Juraj Strossmayer University of Osijek, Faculty of Medicine, Biochemistry and Clinical Chemistry, J. Huttlera 4, 31000 Osijek, Croatia*
[c]*Laboratory for Solid State and Complex Compounds Chemistry, Ruđer Bošković Institute, Division of Materials Chemistry, Bijenička cesta 54, 10 000 Zagreb, Croatia*

*Corresponding authors:
Silvana Raić-Malić, e-mail: sraic@fkit.unizg.hr, Phone: +385 1 459 7213, Fax: +385 1 459 7260
Ljubica Glavaš-Obrovac, email: lgobrovac@mefos.hr, Phone: +385 31 512 800, Fax: +385 31 512 833

Abstract

Novel quinoline **5a–5e** and coumarin **6a–6d** ligands with aldoxime ether linked pyridine moiety were synthesized by *O*-alkylation of quinoline and coumarin with (*E*)-picolinaldehyde oxime and subsequently with [Re(CO)$_5$Cl] gave rhenium(I) tricarbonyl complexes $\mathbf{5a_{Re}}$–$\mathbf{5e_{Re}}$ and $\mathbf{6a_{Re}}$–$\mathbf{6d_{Re}}$ that were fully characterized by NMR, single-crystal X-ray diffraction, IR and UV-Vis spectroscopy. The results of antiproliferative evaluation of quinoline and coumarin ligands and their rhenium(I) tricarbonyl complexes on various human tumor cell lines, including acute lymphoblastic leukemia (CCRF-CEM), acute monocytic leukemia (THP1), cervical adenocarcinoma (HeLa), colon adenocarcinoma (CaCo-2), T-cell lymphoma (HuT78), and non-tumor human fibroblasts (BJ) showed that the quinoline complexes $\mathbf{5a_{Re}}$–$\mathbf{5e_{Re}}$ had higher inhibitory activity than coumarin complexes $\mathbf{6a_{Re}}$–$\mathbf{6d_{Re}}$, particularly against T-cell lymphoma (HuT78) cells. Compounds **5e**, $\mathbf{5e_{Re}}$, **6d** and $\mathbf{6d_{Re}}$ were found to arrest the cell cycle of HuT78 cells by causing a significant accumulation of cells in the G0/G1 phase and a marked decrease in the number of cells in the G2/M phase. These rhenium(I) tricarbonyl complexes also slightly increased ROS production and significantly decreased the mitochondrial membrane potential by 50% ($\mathbf{5e_{Re}}$) and 45% ($\mathbf{6d_{Re}}$) compared to untreated cells and cells treated with **5e** and **6d**. These results suggest that the cytotoxic effects of these compounds are mediated by their effects on mitochondrial membrane potential and the subsequent increase in ROS production.

Keywords: Quinolines, Coumarins, Rhenium(I) complexes, Antiproliferative activity, T-cell Lymphoma, ROS, Mitochondrial membrane potential

1. Introduction

Cancer is a major public health problem worldwide and the second leading cause of death with 20 million new cancer cases and 9.7 million deaths in 2022 [1]. According to the World Health Organization (WHO), about 1 in 5 people will develop cancer in their lifetime and about 1 in 9 men and 1 in 12 women will die from the disease [2]. The incidence of lymphoma, which is the most common lymphoid malignancy, has gradually increased over previous decades, and it ranks among the ten most prevalent cancers worldwide. No effective chemotherapy for adult T-cell leukaemia-lymphoma has yet been established, and the prognosis for patients with this disease is very poor [3]. The development of multidrug resistance and significant side effects are the main contributors to cancer-related mortality, causing the urgent need for new drugs with improved anticancer efficacy and reduced adverse effects [4,5]. Quinoline and cumarin derivatives have been found in many biologically active natural and synthetic compounds, which particularly exhibit anticancer activity [6–9]. These heterocycles have been also used in combination with other pharmacophores by the molecular hybridization strategy that can lead to new candidates with greater safety profiles and improved anti-cancer activity against drug-sensitive and drug-resistant cancers [10]. Quinolines have been recently examined for their modes of action as inhibitors of tyrosine kinases, topoisomerase, proteasome, tubulin polymerization, and DNA repair [11,12]. Some quinoline-bearing compounds have been used as drugs for various cancer treatments (Fig. 1).

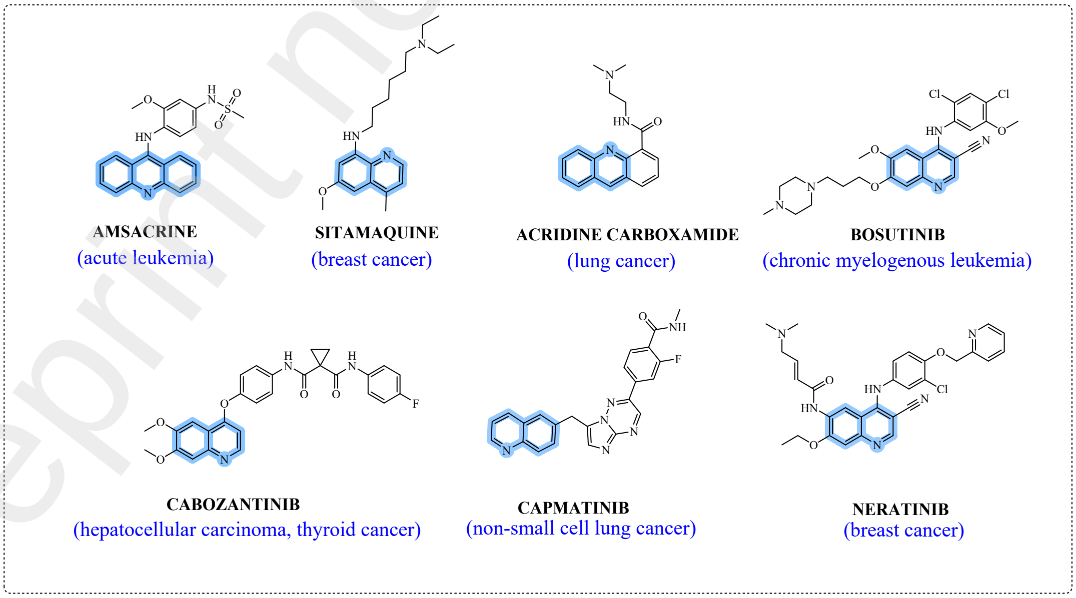

AMSACRINE (acute leukemia)

SITAMAQUINE (breast cancer)

ACRIDINE CARBOXAMIDE (lung cancer)

BOSUTINIB (chronic myelogenous leukemia)

CABOZANTINIB (hepatocellular carcinoma, thyroid cancer)

CAPMATINIB (non-small cell lung cancer)

NERATINIB (breast cancer)

Fig. 1. The quinolone-based compounds in clinical treatment as anticancer drugs.

Over the past two decades, the anticancer potential of coumarin derivatives, their mechanism of action and SAR studies were investigated [10,13–20]. The pharmacological activities of coumarins have been attributed to non-covalent interactions, such as π–π stacking, hydrophobic interactions, electrostatic interactions, hydrogen bonding, metal coordination, and van der Waals forces with active sites of targeted enzymes [17]. On the other hand, organometallic compounds offer new opportunities in the design of novel anticancer drug candidates due to their unique electronic and stereochemical properties and ability to interact with biomolecules [21–24]. Among the various transition metal complexes used in biological applications, quinoline-based complexes have emerged as a promising compounds with significant anticancer activitiy [25]. Recently, Ru(II)/III, Ir(III), Rh(III), Pd(II), Pt(II), Cu(II), Ni(II), Zn(II), Co(II), Au(I), and other complexes containing quinoline have received significant attention because of their promising antiproliferative activity [26,27,36–38,28–35]. These quinoline metal complexes showed different mode of action including proteasome-independent NFκB signaling pathway [39], binding to DNA via intercalation mode [40–42], or inducing apoptosis in cancer cells *via* mitochondrial dysfunction [43–45]. Copper(II) complexes of halogenated quinoline Schiff base derivatives enabled cancer therapy through glutathione-assisted chemodynamic therapy and inhibition of autophagy flux [34]. Quinoline-based Ir(III) complex displayed a superior inhibitory effect on non-small lung (NCI-H460) xenograft in vivo than cisplatin, induced telomerase inhibition and damaged mitochondria in NCI-H460 cells [46]. Additionally, coumarin-palladium(II) complex exhibited remarkable reduction in pancreatic carcinoma cells (PANC-1) growth both *in vitro* and *in vivo* against pancreatic carcinoma cells [47]. Bi-functional platinum(IV) complex with 7-hydroxycoumarin ligands in axial position reduced tumor-associated inflammation by inhibiting cyclooxygenase (COX) [48,49]. Ruthenium(III), copper(II) complexes of 7-methoxy and 8-*tert*-butyl-substituted coumarins, respectively, exhibited *in vitro* cytotoxic effect against cervical cancer cells (HeLa) acting as a groove binding agent [50,51]. Some cobalt(II) complexes of coumarin Schiff bases showed anticancer potential on HeLa cells caused by (that may be a result of) the generation of reactive oxygen species (ROS) [52]. Cobalt(III) complexes of naturally occurring esculetin (6,7-dihydroxycoumarin) as dianionic *O,O*-donor represented an interesting example of potent next-generation photochemotherapeutics [53]. In particular, Re-based complexes have recently drawn interest, mainly due to their ability to modulate the redox status of cancer cells [54–58], thus offering different mechanisms of action such as photoactivity, redox activity, ligand exchange and catalytic activity.

Motivated by the diverse bioactivity of coumarins and quinolones in our previous research [59–66], we present here the synthesis and antiproliferative activity of novel quinoline and coumarin derivatives with aldoxime ether linked pyridine moiety and their $Re[(CO)_3]^+$ metal complexes (Fig. 2).

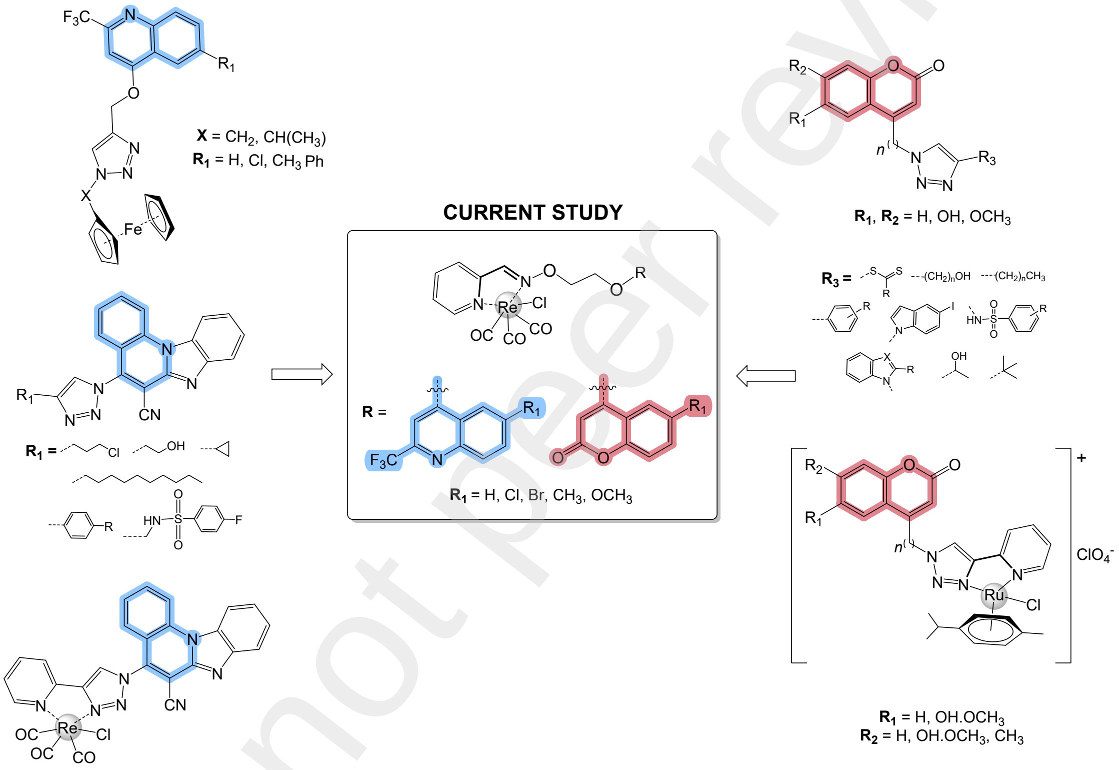

Fig. 2. Rational behind the design of novel quinoline and coumarin-based ligands and rhenium(I) tricarbonyl complexes.

2. Experimental Part

2.1. Materials and methods

All solvents and chemicals (*syn*-pyridine-2-aldoxime **1**, 4-hydroxy-2*H*-chromen-2-one **4a**, 6-chloro-4-hydroxy-2*H*-chromen-2-one **4b**, 6-bromo-4-hydroxy-2*H*-chromen-2-one **4c**, 4-hydroxy-6-methyl-2*H*-chromen-2-one **4d**) were purchased from Aldrich (St. Louis, MO) and Acros (Geel, Belgium). Melting points were determined on a Kofler micro hot-stage (Wien, Austria) and were reported uncorrected. TLC on silica gel 60F-254 plates (Darmstadt, Germany) was used for purity control and reaction monitoring, and the spots were detected under UV light (254 nm). The IR spectra of all compounds were recorded with a PerkinElmer Spectrum ONE FT-IR equipped with a Universal UATR Sampling Accessory covering the range 3500–500 cm^{-1}, while the UV/Vis spectra were measured in acetonitrile (HPLC grade) with a Varian Cary 50 spectrophotometer at 25 °C. Proton (^1H NMR) and carbon (^{13}C NMR) magnetic resonance spectra were recorded using a Bruker (Bruker Biospin, Rheinstetten, Germany) 300 and 600 MHz NMR spectrometer and a Varian INOVA 400 instrument (Palo Alto, SAD) using tetramethylsilane (TMS) as the internal standard in DMSO-d_6 at 298 K. Chemical shifts were referenced to the residual solvent signal of DMSO-d6 at δ 2.50 ppm for ^1H and δ 39.50 ppm for ^{13}C. Elemental composition analyses of all new compounds were within 0.5% of the calculated values.

The quinoline precursors, 2-(trifluoromethyl)quinolin-4-ol **3a**, 6-chloro-2-(trifluoromethyl)quinolin-4-ol **3b**, 6-bromo-2-(trifluoromethyl)quinolin-4-ol **3c**, 6-methyl-2-(trifluoromethyl)quinolin-4-ol **3d** and 6-methoxy-2-(trifluoromethyl)quinolin-4-ol **3e** are known compounds which were synthesized according to the method shown in Scheme S1 (Supplementary Material) [65,67,68].

*2.2. Synthesis of the (E)-picolinaldehyde-O-(2-bromoethyl)oxime (**2**)*

syn-Pyridine-2-aldoxime (5.0 g, 0.041 mol) was dissolved in 100 mL DMF, and NaH (1.5 eq, 2.5 g, 0.062 mol, 60% suspension in mineral oil) was added in small portions at 0 °C. After 60 minutes, 1,2-dibromoethane (1.2 eq, 9.2 g, 0.049 mol) was added and the mixture was stirred overnight in the dark. The solvent was removed under reduced pressure and the residue was purified by column chromatography on silica gel (CH_2Cl_2:CH_3OH = 50:1) to give a yellow oil (5.3 g, 56.4%). ^1H NMR (300 MHz, DMSO) δ 8.62 (d, J = 4.7 Hz, 1H, H-6'), 8.24 (s, 1H, C$\underline{H}$-N), 7.87 – 7.82 (m, 2H, H-3', H-4'), 7.44 (ddd, J = 6.7, 4.9, 1.5 Hz, 1H, H-5'), 4.46 (t, J = 5.7 Hz, 2H, C$\underline{H}_2$), 3.76 (t, J = 5.7 Hz, 2H, C$\underline{H}_2$); ^{13}C NMR (75 MHz, DMSO) δ 150.64, 150.14, 149.67, 136.98, 124.67, 120.80, 73.61, 31.26.

*2.3. General procedure for synthesis of ligands **5a–5e** and **6a–6d***

The corresponding quinoline (**3a–3e)** or coumarin derivative (**4a–4d)** and K_2CO_3 (1.5 eq) were dissolved in DMF and the mixture was stirred for 1h. After this period, (*E*)-picolinaldehyde *O*-(2-bromoethyl) oxime **2** (1.2 eq) was added, and the reaction mixture was stirred overnight at 80 °C. After completion, the reaction mixture was dissolved in CH_2Cl_2 (20 mL) and washed with distilled water (3×20 mL). The organic layer was dried over anhydrous $MgSO_4$, and the solvent was removed under vacuum. The residue was isolated by column chromatography or recrystallized from CH_3OH to afford the pure *O*-alkylated products **5a–5e** and **6a–6d**.

*2.3.1. Synthesis of (E)-picolinaldehyde O-(2-((2-(trifluoromethyl)quinolin-4-yl)oxy)ethyl) oxime (**5a**)*

Compound **5a** was prepared according to the general procedure from 2-(trifluoromethyl)quinolin-4-ol **3a** (100.0 mg, 0.469 mmol), K_2CO_3 (97.3 mg, 0.704 mmol) and (*E*)-picolinaldehyde *O*-(2-bromoethyl) oxime **2** (128.9 mg, 0.563 mmol). Compound **5a** was isolated as a white powder (102.2 mg, 60.3%, m.p. = 91–93 °C). ^{1}H NMR (300 MHz, DMSO) δ 8.60 (d, *J* = 4.6 Hz, 1H, H-6'), 8.30 – 8.20 (m, 2H, C$\underline{H}$-N, H-5), 8.08 (d, *J* = 8.4 Hz, 1H, H-8), 7.91 – 7.77 (m, 3H, H-7, H-6, H-4'), 7.68 (t, *J* = 7.5 Hz, 1H, H-3'), 7.47 (s, 1H, H-3), 7.45 – 7.38 (m, 1H, H-5'), 4.73 (d, *J* = 4.6 Hz, 2H, C$\underline{H_2}$), 4.69 (d, *J* = 4.5 Hz, 2H, C$\underline{H_2}$); ^{13}C NMR (75 MHz, DMSO) δ 162.72, 150.73, 149.91, 149.63, 148.57, 147.90 (q, *J* = 33.6 Hz), 136.86, 131.38, 129.06, 127.97, 124.56, 121.81, 121.47 (q, *J* = 275.7 Hz), 121.10, 120.61, 97.79, 72.25, 68.08; IR (ATR) /cm^{-1}: 3073, 2946, 2988, 2030, 1592, 1575, 1512, 1470, 1387, 1352, 1279, 1254, 1181, 1089, 1086, 1041, 1181, 1086, 1041, 969, 944, 831, 775, 724, 620; Calc. for $C_{18}H_{14}F_3N_3O_2$ (Mr = 361.3) C, 59.83; H, 3.91; F, 15.77; N, 11.63; found: C, 59.89; H, 3.87; F, 15.70; N, 11.71%.

*2.3.2. Synthesis of (E)-picolinaldehyde O-(2-((6-chloro-2-(trifluoromethyl)quinolin-4-yl)oxy)ethyl) oxime (**5b**)*

Compound **5b** was prepared according to the general procedure from 6-chloro-2-(trifluoromethyl)quinolin-4-ol **3b** (100.0 mg, 0.404 mmol), K_2CO_3 (83.7 mg, 0.606 mmol) and (*E*)-picolinaldehyde *O*-(2-bromoethyl) oxime **2** (111.1 mg, 0.485 mmol). Compound **5b** was isolated as a white powder (130.7 mg, 81.6%, m.p. = 91–93 °C). ^{1}H NMR (300 MHz, DMSO) δ 8.59 (d, *J* = 4.5 Hz, 1H, H-6'), 8.22 (s, 1H, C$\underline{H}$-N), 8.19 (d, *J* = 2.3 Hz, 1H, H-5), 8.10 (d, *J* = 9.0 Hz, 1H, H-8), 7.88 (dd, *J* = 9.0, 2.3 Hz, 1H, H-7), 7.81 (dt, *J* = 15.2, 4.5 Hz, 2H, H-3', H-4'), 7.54 (s, 1H, H-3), 7.45 – 7.39 (m, 1H, H-5'), 4.74 (d, *J* = 4.7 Hz, 2H, C$\underline{H_2}$), 4.70 (d, J = 4.7 Hz, 2H, C$\underline{H_2}$); ^{13}C NMR (151 MHz, DMSO) δ 162.02, 150.71, 149.90, 149.65, 148.38 (q, *J* = 33.9 Hz), 145.83, 136.89, 132.76, 131.97, 131.37, 124.56, 121.96, 121.32 (q, *J* = 275.7 Hz), 120.71, 120.54, 98.81, 72.13, 68.59; IR (ATR) /cm^{-1}: 3079, 2981, 2885, 2027, 1918, 1717, 1588, 1459, 1392, 1356, 1274, 1177, 1131, 1086, 977, 851, 781, 728; Calc. for $C_{18}H_{13}ClF_3N_3O_2$ (Mr = 395.8) C, 54.63; H, 3.31; Cl, 8.96; F, 14.40; N, 10.62; found: C, 54.69; H, 3.38; Cl, 8.92; F, 14.46; N, 10.63%.

*2.3.3. Synthesis of (E)-picolinaldehyde O-(2-((6-bromo-2-(trifluoromethyl)quinolin-4-yl)oxy)ethyl) oxime (**5c**)*

Compound **5c** was prepared according to the general procedure from 6-bromo-2-(trifluoromethyl)quinolin-4-ol **3c** (200.0 mg, 0.685 mmol), K_2CO_3 (142.0 mg, 1.028 mmol) and (*E*)-picolinaldehyde *O*-(2-bromoethyl) oxime **2** (188.3 mg, 0.822 mmol). Compound **5c** was isolated as a white powder (185.1 mg, 61.4%, m.p. = 153–155 °C). ^{1}H NMR (300 MHz, DMSO) δ 8.60 (d, J = 4.5 Hz, 1H, H-6’), 8.37 (d, J = 1.4 Hz, 1H, H-5), 8.23 (s, 1H, C$\underline{H}$-N), 8.02 (dd, J = 7.7, 5.4 Hz, 2H, H-7, H-8), 7.93 – 7.75 (m, 2H, H-4’, H-3’), 7.55 (s, 1H, H-3), 7.47 – 7.38 (m, 1H, H-5’), 4.75 (d, J = 4.7 Hz, 2H, C$\underline{H}_2$), 4.70 (d, J = 4.7 Hz, 2H, C$\underline{H}_2$); ^{13}C NMR (75 MHz, DMSO) δ 161.89, 150.70, 149.92, 149.66, 148.37 (q, J = 33.8 Hz), 146.00, 136.92, 134.53, 131.37, 124.57, 123.96, 122.37, 120.89 (q, J = 275.7 Hz), 120.53, 120.35, 98.80, 72.13, 68.61; IR (ATR) /cm^{-1}: 3035, 2962, 2026, 1926, 1720, 1588, 1457, 1391, 1355, 1272, 1176, 1087, 979, 941, 937, 830, 782, 757, 620; Calc. for $C_{18}H_{13}BrF_3N_3O_2$ (Mr = 440.2) C, 49.11; H, 2.98; Br, 18.15; F, 12.95; N, 9.55; found: C, 49.07; H, 2.83; Br, 18.19; F, 12.91; N, 9.61%.

*2.3.4. Synthesis of (E)-picolinaldehyde O-(2-((6-methyl-2-(trifluoromethyl)quinolin-4-yl)oxy)ethyl) oxime (**5d**)*

Compound **5d** was prepared according to the general procedure from 6-methyl-2-(trifluoromethyl)quinolin-4-ol **3d** (150.0 mg, 0.660 mmol), K_2CO_3 (136.8 mg, 0.990 mmol) and (*E*)-picolinaldehyde *O*-(2-bromoethyl) oxime **2** (181.4 mg, 0.792 mmol). Compound **5d** was isolated as a white powder (101.8 mg, 41.1%, m.p. = 122–123 °C). ^{1}H NMR (300 MHz, DMSO) δ 8.60 (d, J = 4.6 Hz, 1H, H-6’), 8.23 (s, 1H, C$\underline{H}$-N), 7.97 (d, J = 9.0 Hz, 2H, H-8/H-5), 7.88 – 7.77 (m, 2H, H-3’, H-4’), 7.70 (dd, J = 8.6, 1.7 Hz, 1H, H-7), 7.46 – 7.40 (m, 2H, H-3, H-5’), 4.70 (d, J = 2.1 Hz, 4H, C$\underline{H}_2$), 2.46 (s, 3H, C$\underline{H}_3$); ^{13}C NMR (151 MHz, DMSO) δ 162.09, 150.76, 149.85, 149.65, 146.97 (q, J = 33.4 Hz), 145.93, 137.93, 136.88, 133.44, 128.87, 124.57, 121.57 (q, J = 275.5 Hz), 121.05, 120.62, 120.40, 97.75, 72.26, 68.08, 21.24; IR (ATR) /cm^{-1}: 3076, 2980, 1687, 1455, 1371, 1247, 1105, 981, 825; Calc. for $C_{19}H_{16}F_3N_3O_2$ (Mr = 375.4) C, 60.80; H, 4.30; F, 15.18; N, 11.20; found: C, 60.78; H, 4.37; F, 15.24; N, 11.24%.

*2.3.5. Synthesis of (E)-picolinaldehyde O-(2-((6-methoxy-2-(trifluoromethyl)quinolin-4-yl)oxy)ethyl) oxime (**5e**)*

Compound **5e** was prepared according to the general procedure from 6-methoxy-2-(trifluoromethyl)quinolin-4-ol **3e** (150.0 mg, 0.617 mmol), K_2CO_3 (127.9 mg, 0.926 mmol) and (*E*)-picolinaldehyde *O*-(2-bromoethyl) oxime **2** (169.6 mg, 0.740 mmol). Compound **5e** was isolated as white powder (134.9 mg, 55.9%, m.p. = 119–122 °C). ^{1}H NMR (300 MHz, DMSO) δ 8.60 (d, *J* = 4.6 Hz, 1H, H-6'), 8.23 (s, 1H, C<u>H</u>-N), 8.00 (d, *J* = 9.1 Hz, 1H, H-5), 7.85 – 7.73 (m, 2H, H-3', H-4'), 7.52 – 7.40 (m, 4H, H-3, H-7, H-8, H-5'), 4.71 (d, *J* = 5.5 Hz, 4H, C$\underline{H_2}$), 3.82 (s, 3H, C$\underline{H_3}$); ^{13}C NMR (151 MHz, DMSO) δ 162.09, 150.76, 149.84, 149.65, 146.96 (q, *J* = 33.3 Hz), 137.92, 136.87, 133.43, 128.87, 124.56, 121.44 (q, *J* = 275.5 Hz), 121.04, 120.65, 120.58, 120.40, 97.74, 72.26, 68.08, 21.24; IR (ATR) /cm^{-1}: 2982, 2024, 1916, 1481, 1283, 1178, 1099, 951, 853, 777; Calc. for $C_{19}H_{16}F_3N_3O_3$ (Mr = 391.4) C, 58.31; H, 4.12; F, 14.56; N, 10.74; found: C, 58.26; H, 4.17; F, 14.62; N, 10.79%.

*2.3.6. Synthesis of (E)-picolinaldehyde O-(2-((2-oxo-2H-chromen-4-yl)oxy)ethyl) oxime (**6a**)*

Compound **6a** was prepared according to the general procedure from 4-hydroxy-2*H*-chromen-2-one **4a** (250.0 mg, 1.542 mmol), K_2CO_3 (319.7 mg, 2.313 mmol) and (*E*)-picolinaldehyde *O*-(2-bromoethyl) oxime **2** (423.9 mg, 1.850 mmol). Compound **6a** was isolated as white powder (279.6 mg, 58.4%, m.p. = 123–125 °C).^{1}H NMR (300 MHz, DMSO) δ 8.61 (d, *J* = 4.6 Hz, 1H, H-6'), 8.24 (s, 1H, C<u>H</u>-N), 7.89 – 7.78 (m, 3H, H-3', H-4', H-5), 7.68 – 7.61 (m, 1H, H-7), 7.45 – 7.37 (m, 2H, H-8, H-5'), 7.31 (t, *J* = 7.6 Hz, 1H, H-6), 5.99 (s, 1H, H-3), 4.62 (d, *J* = 4.9 Hz, 2H, C$\underline{H_2}$), 4.56 (d, *J* = 4.9 Hz, 2H, C$\underline{H_2}$); ^{13}C NMR (75 MHz, DMSO) δ 164.70, 161.52, 152.73, 150.72, 149.93, 149.64, 136.89, 132.74, 124.58, 124.08, 122.85, 120.64, 116.39, 115.08, 90.86, 71.83, 68.19; IR (ATR) /cm^{-1}: 3080, 2982, 2938, 1714, 1699, 1622, 1566, 1411, 1383, 1274, 1249, 1191, 1143, 1078, 1067, 930, 855, 765; Calc. for $C_{17}H_{14}N_2O_4$ (Mr = 310.3) C, 65.80; H, 4.55; N, 9.03; found: C, 65.76; H, 4.56; N, 9.07%.

*2.3.7. Synthesis of (E)-picolinaldehyde O-(2-((6-chloro-2-oxo-2H-chromen-4-yl)oxy)ethyl) oxime (**6b**)*

Compound **6b** was prepared according to the general procedure from 6-chloro-4-hydroxy-2*H*-chromen-2-one **4b** (100.0 mg, 0.509 mmol), K_2CO_3 (105.5 mg, 0.763 mmol) and (*E*)-picolinaldehyde *O*-(2-bromoethyl) oxime **2** (139.9 mg, 0.611 mmol). Compound **6b** was isolated as white powder (87.7 mg, 50.0 %, m.p. = 187–189 °C). ^{1}H NMR (600 MHz, DMSO) δ 8.61 – 8.60 (m, 1H, H-6'), 8.25 (s, 1H, C<u>H</u>-N), 7.86 – 7.83 (m, 1H, H-4'), 7.80 (dd, *J* = 6.7, 1.3 Hz, 1H, 3'), 7.75 (d, *J* = 2.5 Hz, 1H, H-5), 7.68 (dt, *J* = 8.2, 1.4 Hz, 1H, H-7), 7.45 (d, *J* = 8.9 Hz, 1H, H-8), 7.44 – 7.41 (m, 1H, H-5'), 6.06 (s, 1H, H-3), 4.65 – 4.62 (m, 2H, CH_2), 4.54 (dd, *J* = 5.1, 3.6 Hz, 2H, CH_2); ^{13}C NMR (151 MHz, DMSO) δ 163.57, 161.12, 151.40, 150.72, 149.95, 149.70, 136.96, 132.48, 128.23, 124.62, 122.00, 120.61, 118.66, 116.61, 91.77, 71.74, 68.69; IR (ATR) /cm^{-1} 3078, 2978, 2940, 1702, 1622, 1559, 1443, 1368, 1185, 1147, 1111, 1079, 984, 940, 860, 824, 705, 531; Calc. for $C_{17}H_{13}ClN_2O_4$ (344.7) C, 59.23; H, 3.80; Cl, 10.28; N, 8.13; found: C, 59.28; H, 3.86; Cl, 10.27; N, 8.08%.

*2.3.8. Synthesis of (E)-picolinaldehyde O-(2-((6-bromo-2-oxo-2H-chromen-4-yl)oxy)ethyl) oxime **(6c)***

Compound **6c** was prepared according to the general procedure from 6-bromo-4-hydroxy-2*H*-chromen-2-one **4c** (200.0 mg, 0.830 mmol), K_2CO_3 (172.0 mg, 1.245 mmol) and (*E*)-picolinaldehyde *O*-(2-bromoethyl) oxime **2** (228.2 mg, 0.996 mmol). Compound **6c** was isolated as white powder (155.0 mg, 48.0 %, m.p. = 188–190 °C). ^{1}H NMR (600 MHz, DMSO) δ 8.61 (ddd, *J* = 4.8, 1.7, 1.0 Hz, 1H, H-6'), 8.25 (s, 1H, C<u>H</u>-N), 7.89 (d, *J* = 2.4 Hz, 1H, H-5), 7.86 (td, *J* = 7.6, 1.5 Hz, 1H, H-4'), 7.82 – 7.78 (m, 2H, H-3', H-7), 7.42 (ddd, *J* = 7.5, 4.8, 1.2 Hz, 1H, H-5'), 7.39 (d, *J* = 8.8 Hz, 1H, H-8), 6.05 (s, 1H, H-3), 4.65 – 4.62 (m, 2H, $C\underline{H}_2$), 4.56 – 4.53 (m, 2H, $C\underline{H}_2$).; ^{13}C NMR (75 MHz, DMSO) *δ* 163.46, 161.01, 151.79, 150.70, 149.94, 149.67, 136.94, 135.22, 124.90, 124.58, 120.55, 118.87, 117.00, 115.92, 91.71, 71.72, 68.68; IR (ATR) /cm^{-1}: 2982, 2882, 1727, 1708, 1619, 1560, 1434, 1349, 1242, 1180, 1086, 968, 882, 778, 705, 516; Calc. for $C_{17}H_{13}BrN_2O_4$ (Mr = 389.2) C, 52.46; H, 3.37; Br, 20.53; N, 7.20; found: C, 52.53; H, 3.28; Br, 20.57; N, 7.25%.

2.3.9. *Synthesis of (E)-picolinaldehyde O-(2-((6-methyl-2-oxo-2H-chromen-4-yl)oxy)ethyl) oxime **(6d)***

Compound **6d** was prepared according to the general procedure from 4-hydroxy-6-methyl-2*H*-chromen-2-one **4d** (200.0 mg, 1.135 mmol), K_2CO_3 (235.4 mg, 1.703 mmol) and (*E*)-picolinaldehyde *O*-(2-bromoethyl) oxime **2** (312.0 mg, 1.362 mmol). Compound **6d** was isolated as white powder (155.0 mg, 42.1 %, m.p. = 171–173 °C). ^{1}H NMR (300 MHz, DMSO) δ 8.61 (d, *J* = 4.7 Hz, 1H, H-6'), 8.25 (s, 1H, C<u>H</u>-N), 7.84 (m, 2H, H-3', H-4'), 7.57 (s, 1H, H-5), 7.45 (dd, *J*

= 5.9, 3.9 Hz, 2H, H-7, H-5'), 7.28 (d, *J* = 8.4 Hz, 1H, H-8), 5.95 (s, 1H, H-3), 4.67 – 4.58 (m, 2H, C<u>H</u>$_2$), 4.53 (d, *J* = 3.8 Hz, 2H, C<u>H</u>$_2$), 2.28 (s, 3H C<u>H</u>$_3$); ^{13}C NMR (75 MHz, DMSO) δ 164.74, 161.71, 150.92, 150.77, 149.90, 149.69, 136.94, 133.59, 133.44, 124.62, 122.33, 120.64, 116.25, 114.80, 90.81, 71.86, 68.30, 20.26; IR (ATR) /cm^{-1}:2971, 2956, 2936, 1571, 1391, 1355, 1273, 1254, 1174, 1130, 1085, 979, 945, 820, 781, 737, 620, 514; Calc. for $C_{18}H_{16}N_2O$ (Mr = 324.3) C, 66.66; H, 4.97; N, 8.64; found: C, 66.62; H, 4.99; N, 8.69%.

*2.4. General procedure for the synthesis of metal complexes **5a$_{Re}$–5e$_{Re}$** and **6a$_{Re}$–6d$_{Re}$***

A solution of $Re(CO)_5Cl$ (1 eq) and corresponding ligand (1 eq) in chloroform (5 mL) was refluxed for 10 h in the dark. The resulting clear yellow solution was cooled to room temperature and its volume was reduced to give a fine yellow precipitate which was collected by filatration and dried.

*2.4.1. Synthesis of complex **5a$_{Re}$***

Compound **5a$_{Re}$** was prepared according to the general procedure from ligand **5a** (30.0 mg, 0.083 mmol) and $Re(CO)_5Cl$ (30.0 mg, 0.083 mmol). Complex **5a$_{Re}$** was isolated as a yellow powder (26.0 mg, 46.9%, m.p. = 132–134 °C). ^{1}H NMR (300 MHz, DMSO) δ 9.46 (s, 1H, C<u>H</u>-N), 9.03 (d, *J* = 5.4 Hz, 1H, H-6'), 8.31 (m, 1H, H-5), 8.23 (d, *J* = 8.3 Hz, 1H, H-8), 8.12 (dd, *J* = 11.3, 7.9 Hz, 2H, H-4', H-7), 7.88 (t, *J* = 7.7 Hz, 1H, H-3'), 7.82 – 7.76 (m, 1H, H-6), 7.64 (t, *J* = 7.6 Hz, 1H, H-5'), 7.50 (s, 1H, H-3), 4.89 (dd, *J* = 13.0, 6.3 Hz, 4H, C<u>H</u>$_2$); ^{13}C NMR (151 MHz, DMSO) δ 196.49, 196.25, 186.87, 162.46, 160.81, 153.26, 151.91, 147.89 (q, *J* = 33.7 Hz), 147.37, 140.58, 131.46, 129.08 (d, *J* = 3.6 Hz), 128.97, 127.91, 121.81, 121.46 (q, *J* = 275.7 Hz), 121.03, 97.86, 79.14, 73.74, 66.77; IR $_{max}$/cm^{-1} 3006, 2981, 2019 (M–C≡O sym. stretch), 1922 (M–C≡O asym. stretch), 1884 (M–C≡O asym. stretch), 1576, 1515, 1475, 1413, 1382, 1348, 1275, 1183, 1182, 1135, 1098, 1044, 991, 942, 769; Calc. for $C_{21}H_{14}ClF_3N_3O_5Re$ (Mr = 667.0) C, 37.82; H, 2.12; Cl, 5.31; F, 8.54; N, 6.30; Re, 27.92; found: C, 37.86; H, 2.18; Cl, 5.26; F, 8.59; N, 6.26; Re, 27.88%.

*2.4.2. Synthesis of complex **5b$_{Re}$***

Compound **5b$_{Re}$** was prepared according to the general procedure from ligand **5b** (30.0 mg, 0.076 mmol) and $Re(CO)_5Cl$ (27.4 mg, 0.076 mmol). Complex **5b$_{Re}$** was isolated as a yellow powder (33.2 mg, 62.5%, m.p. = 131–133 °C). ^{1}H NMR (300 MHz, DMSO) *δ* 9.47 (s, 1H, C<u>H</u>-N), 9.03 (d, *J* = 5.2 Hz, 1H, H-6'), 8.31 (dd, *J* = 8.4, 7.2 Hz, 1H, H-4'), 8.16 – 8.10 (m, 3H, H-5, H-8, H-3'), 7.88 (dd, *J* = 9.0, 2.4 Hz, 1H, H-7), 7.80 (dd, *J* = 5.3, 3.5 Hz, 1H, H-5'), 7.57 (s, 1H, H-3), 4.95 – 4.90 (m, 2H, C<u>H</u>$_2$), 4.91 – 4.86 (m, 2H, C<u>H</u>$_2$); ^{13}C NMR (151 MHz, DMSO) δ 196.52, 196.24, 186.85, 161.76, 151.88, 148.34 (q, *J* = 33.9 Hz), 145.82, 140.62, 132.82, 132.01, 131.32, 129.14, 128.98, 121.84, 121.32 (d, *J* = 275.7 Hz), 120.81, 98.81, 73.47, 72.46, 67.46, 63.05; IR (ATR) /cm^{-1}: 2981, 2988, 2020 (M–C≡O sym. stretch), 1940 (M–C≡O asym. stretch), 1893 (M–C≡O asym. stretch), 1723, 1577, 1573, 1465, 1463, 1388, 1354, 1276, 1252, 1186, 1127, 1098, 982, 830,779, 728; Calc. for $C_{21}H_{13}Cl_2F_3N_3O_5Re$ (Mr = 701.5) C, 35.96; H, 1.87; Cl, 10.11; F, 8.13; N, 5.99; Re, 26.55; found: C, 35.99; H, 1.91; Cl, 10.16; F, 8.19; N, 5.96; Re, 26.60%.

2.4.3. Synthesis of complex ***5c**$_{Re}$*

Compound **5c**$_{\mathbf{Re}}$ was prepared according to the general procedure from ligand **5c** (20.0 mg, 0.046 mmol) and Re(CO)$_5$Cl (16.4 mg, 0.046 mmol). Complex **5c**$_{\mathbf{Re}}$ was isolated as a yellow powder (23.0 mg, 67.0%, m.p. = 143–145 °C). ^{1}H NMR (600 MHz, DMSO) δ 9.47 (s, 1H, C$\underline{H}$-N), 9.03 (d, *J* = 5.3 Hz, 1H, H-6'), 8.31 (ddd, *J* = 9.2, 6.0, 1.9 Hz, 2H, H-5, H-4'), 8.12 (d, *J* = 7.6 Hz, 1H, H-3'), 8.00 (dt, *J* = 9.0, 5.6 Hz, 2H, H-8, H-7), 7.79 (ddd, *J* = 7.7, 5.4, 1.4 Hz, 1H, H-5'), 7.56 (s, 1H, H-3), 4.97 – 4.90 (m, 2H, C$\underline{H}_2$), 4.87 (dd, *J* = 7.2, 3.3 Hz, 2H, C$\underline{H}_2$); ^{13}C NMR (151 MHz, DMSO) δ 196.56, 196.26, 186.86, 161.65, 161.18, 153.37, 151.88, 148.41 (q, *J* = 33.7 Hz), 122.26, 146.01, 140.64, 134.61, 131.33, 129.20, 129.01, 124.06, 121.84, 121.85 (q, *J* = 124.1 Hz), 98.84, 73.47, 67.50; IR (ATR) /cm^{-1}: 2981, 2936, 2024 (M–C≡O sym. stretch), 1893 (M–C≡O asym. stretch), 1588, 1458, 1391, 1356, 1275, 1135, 1088, 980, 945, 884, 851, 781; Calc. for $C_{21}H_{13}Cl_2BrF_3N_3O_5Re$ (Mr = 744.9) C, 33.82; H, 1.76; Br, 10.71; Cl, 4.75; F, 7.64; N, 5.63; Re, 24.96; found: C, 33.89; H, 1.82; Br, 10.79; Cl, 4.81; F, 7.61; N, 5.60; Re, 24.99%.

2.4.4. Synthesis of complex ***5d**$_{Re}$*

Compound **5d**$_{\mathbf{Re}}$ was prepared according to the general procedure from ligand **5d** (30.0 mg, 0.079 mmol) and Re(CO)$_5$Cl (28.9 mg, 0.079 mmol). Complex **5d**$_{\mathbf{Re}}$ was isolated as a yellow powder (28.5 mg, 53.0%, m.p. = 122–123 °C). ^{1}H NMR (300 MHz, DMSO) δ 9.46 (s, 1H, C$\underline{H}$-N), 9.04 (d, *J* = 5.1 Hz, 1H, H-6'), 8.31 (dd, *J* = 7.7, 6.6 Hz, 1H, H-4'), 8.11 (d, *J* = 7.6 Hz, 1H, H-3'), 7.98 (d, *J* = 8.2 Hz, 2H, H-8, H-5), 7.86 – 7.75 (m, 1H, H-5'), 7.70 (dd, *J* = 8.7, 1.6 Hz, 1H, H-7), 7.44 (s, 1H, H-3), 4.99 – 4.88 (m, 2H, C$\underline{H}_2$), 4.88 – 4.79 (m, 2H, C$\underline{H}_2$), 2.38 (s, 3H, C$\underline{H}_3$); ^{13}C NMR (151 MHz, DMSO) *δ* 196.53, 196.24, 186.89, 161.82, 160.87, 153.30, 151.96, 146.95 (q, *J* = 33.5 Hz), 145.93, 140.62, 137.89, 133.44, 129.10, 128.94, 128.82, 120.95, 120.53, 119.46 (q, *J* = 33.5 Hz), 97.76, 73.66, 66.97, 21.20; IR (ATR) /cm^{-1}: 3074, 2982, 2930, 2024 (M–C≡O sym. stretch), 1908 (M–C≡O asym. stretch), 187 (M–C≡O asym. stretch), 1357, 1282, 1233, 1178, 1100, 1099, 951, 835, 735, 714; Calc. for $C_{22}H_{16}ClF_3N_3O_5Re$ (Mr = 681.0) C, 38.80; H, 2.37; Cl, 5.21; F, 8.37; N, 6.17; Re, 27.34; found: C, 38.84; H, 2.40; Cl, 5.25; F, 8.41; N, 6.14; Re, 27.38%.

2.4.5. Synthesis of complex ***5e***$_{\mathbf{Re}}$

Compound **5e**$_{\mathbf{Re}}$ was prepared according to the general procedure from ligand **5e** (20.0 mg, 0.051 mmol) and $Re(CO)_5Cl$ (18.5 mg, 0.051 mmol). Complex **5e**$_{\mathbf{Re}}$ was isolated as a yellow powder (32.0 mg, 89.8 %, m.p. = 122–123 °C).^{1}H NMR (600 MHz, DMSO) δ 9.46 (s, 1H, CH-N), 9.04 (dd, *J* = 5.4, 1.5 Hz, 1H, H-6'), 8.30 (td, *J* = 7.8, 1.7 Hz, 1H, H-4'), 8.11 (dd, *J* = 7.7, 1.2 Hz, 1H, H-3'), 7.97 (m, 2H, H-5, H-8), 7.81 – 7.77 (m, 1H, H-5'), 7.70 (dd, *J* = 8.5, 2.1 Hz, 1H, H-7), 7.44 (s, 1H, H-Ar), 4.95 – 4.89 (m, 2H, C$\underline{H}_2$), 4.89 – 4.71 (m, 2H, C$\underline{H}_2$), 2.37 (s, 3H, C$\underline{H}_3$);^{13}C NMR (151 MHz, DMSO) *δ* 196.54, 196.25, 186.91, 161.84, 160.89, 153.32, 151.97, 146.96 (q, *J* = 33.5 Hz), 145.94, 140.63, 137.91, 133.46, 129.12, 128.95, 128.84, 121.58 (q, *J* = 275.4 Hz), 120.96, 120.55, 97.78, 73.66, 66.99, 21.21; IR (ATR) /cm^{-1}: 3072, 2981, 2929, 2022 (M–C≡O sym. stretch), 1914 (M–C≡O asym. stretch), 1896 (M–C≡O asym. stretch), 1358, 1282, 1233, 1178, 1100, 1099, 951, 835, 735, 715; Calc. for $C_{22}H_{16}ClF_3N_3O_6Re$ (Mr = 697.0) C, 37.91; H, 2.31; Cl, 5.09; F, 8.18; N, 6.03; Re, 26.71; found: C, 37.98; H, 2.26; Cl, 5.13; F, 8.22; N, 6.01; Re, 26.66%.

2.4.6. Synthesis of complex ***6a***$_{\mathbf{Re}}$

Compound **6a**$_{\mathbf{Re}}$ was prepared according to the general procedure from ligand **6a** (50.0 mg, 0.161 mmol) and $Re(CO)_5Cl$ (58.2 mg, 0.161 mmol). Complex **6a**$_{\mathbf{Re}}$ was isolated as a yellow powder (87.7 mg, 88.4%, m.p. > 250 °C). ^{1}H NMR (300 MHz, DMSO) δ 9.46 (s, 1H, C$\underline{H}$-N), 9.02 (d, *J* = 5.1 Hz, 1H, H-6'), 8.31 (t, *J* = 7.6 Hz, 1H, H-4'), 8.15 (d, *J* = 7.6 Hz, 1H, H-3'), 7.80 (d, *J* = 7.7 Hz, 2H, H-5, H-5'), 7.64 (t, *J* = 7.6 Hz, 1H, H-7), 7.40 (d, *J* = 8.2 Hz, 1H, H-8), 7.26 (t, *J* = 7.6 Hz, 1H, H-6), 5.99 (s, 1H, H-3), 4.83 (s, 2H, C$\underline{H}_2$), 4.69 (s, 2H, C$\underline{H}_2$);^{13}C NMR (75 MHz, DMSO) δ 196.48, 196.24, 186.85, 164.48, 161.46, 160.97, 153.25, 152.74, 151.87, 140.58, 132.82, 129.09, 129.00, 123.98, 122.86, 116.44, 114.98, 91.09, 73.40, 66.82; IR (ATR) /cm^{-1}: 2997, 2982, 2026 (M–C≡O sym. stretch), 1912 (M–C≡O asym. stretch), 1726, 1625, 1411, 1237, 1178, 1049, 1047, 931, 805, 772, 640; Calc. for $C_{20}H_{14}ClN_2O_7Re$ (Mr = 616.0) C, 39.00; H, 2.29; Cl, 5.75; N, 4.55; Re, 30.23; found: C, 39.06; H, 2.35; Cl, 5.80; N, 4.59 Re, 30.27%.

2.4.7. Synthesis of complex ***6b***$_{\mathbf{Re}}$

Compound **6b**$_{\mathbf{Re}}$ was prepared according to the general procedure from ligand **6b** (30.0 mg, 0.087 mmol) and $Re(CO)_5Cl$ (31.4 mg, 0.087 mmol). Complex **6b**$_{\mathbf{Re}}$ was isolated as a yellow powder

(31.9 mg, 56.4%, m.p. = 115–117 °C). ^{1}H NMR (300 MHz, DMSO) δ 9.48 (s, 1H, $\mathrm{C\underline{H}}$-N), 9.02 (d, *J* = 5.2 Hz, 1H, H-6'), 8.31 (t, *J* = 7.2 Hz, 1H, H-4'), 8.13 (d, *J* = 7.7 Hz, 1H, H-3'), 7.85 (d, *J* = 2.3 Hz, 1H, H-5), 7.82 – 7.75 (m, 2H, H-5', H-7), 7.38 (d, *J* = 8.8 Hz, 1H, H-8), 6.06 (s, 1H, H-3), 4.85 (m, 2H, $\mathrm{C\underline{H}_2}$), 4.69 (m, 2H, $\mathrm{C\underline{H}_2}$); ^{13}C NMR (151 MHz, DMSO) δ 198.52, 198.21, 188.82, 165.27, 163.30, 162.96, 155.33, 153.79, 142.61, 137.27, 131.19, 131.01, 134.01, 127.03, 120.80, 118.84, 117.95, 93.92, 75.14, 69.51; IR (ATR) /cm^{-1}: 3034, 2017 (M–C≡O sym. stretch), 1918 (M–C≡O asym. stretch), 1882 (M–C≡O asym. stretch), 159, 1057, 1501, 1458, 1389, 1350, 1277, 1192, 1136, 947, 846, 772, 643. Calc. for $C_{20}H_{13}Cl_2N_2O_7Re$ (Mr = 650.4) C, 36.93; H, 2.01; Cl, 10.90; N, 4.31; Re, 28.63; found: 36.99; H, 2.07; Cl, 10.96; N, 4.35; Re, 28.58%.

2.4.8. Synthesis of complex **6c**$_{\mathbf{Re}}$

Compound **6c**$_{\mathbf{Re}}$ was prepared according to the general procedure from ligand **6c** (50.0 mg, 0.128 mmol) and $Re(CO)_5Cl$ (46.4 mg, 0.128 mmol). Complex **6c**$_{\mathbf{Re}}$ was isolated as a yellow powder (36.2 mg, 40.7%, m.p. = 247–249 °C). ^{1}H NMR (300 MHz, DMSO) δ 9.48 (s, 1H, $\mathrm{C\underline{H}}$-N), 9.03 (d, *J* = 5.2 Hz, 1H, H-6'), 8.31 (t, *J* = 7.2 Hz, 1H, H-4'), 8.14 (d, *J* = 7.7 Hz, 1H, H-3'), 7.85 (d, *J* = 2.3 Hz, 1H, H-5), 7.82 – 7.75 (m, 2H, H-7, H-5'), 7.38 (d, *J* = 8.8 Hz, 1H, H-8), 6.06 (s, 1H, H-3), 4.86 (s, 2H, $\mathrm{C\underline{H}_2}$), 4.69 (s, 2H, $\mathrm{C\underline{H}_2}$); ^{13}C NMR (151 MHz, DMSO) δ 196.52, 196.21, 186.82, 163.27, 161.30, 160.96, 153.33, 151.28, 151.75, 140.61, 135.27, 129.19, 129.01, 125.03, 118.80, 116.84, 115.95, 91.92, 73.14, 67.51; IR (ATR) /cm^{-1}: 3008, 2981, 2884, 2028 (M–C≡O sym. stretch), 1907 (M–C≡O asym. stretch), 1728, 1709, 1561, 1434, 1350, 1243, 1186, 1081, 968, 822, 705, 657; Calc. for $C_{20}H_{13}BrClN_2O_7Re$ (Mr = 694.9) C, 34.57; H, 1.89; Br, 11.50; Cl, 5.10; N, 4.03; Re, 26.80; found: C, 34.61; H, 1.84; Br, 11.54; Cl, 5.16; N, 4.09; Re, 26.86%.

2.4.9. Synthesis of complex **6d**$_{\mathbf{Re}}$

Compound **6d**$_{\mathbf{Re}}$ was prepared according to the general procedure from ligand **6d** (20.0 mg, 0.062 mmol) and $Re(CO)_5Cl$ (22.3 mg, 0.062 mmol). Complex **6d**$_{\mathbf{Re}}$ was isolated as a yellow powder (20.9 mg, 53.5%, m.p. = 247–249 °C). ^{1}H NMR (600 MHz, DMSO) δ 9.48 (s, 1H, $\mathrm{C\underline{H}}$-N), 9.07 – 8.96 (m, 1H, H-6'), 8.31 (td, *J* = 7.8, 1.4 Hz, 1H, H-Ar, H-4'), 8.13 (d, *J* = 7.5 Hz, 1H, H-3'), 7.79 (ddd, *J* = 7.7, 5.4, 1.4 Hz, 1H, H-5'), 7.56 (d, *J* = 1.2 Hz, 1H, H-5), 7.44 (dd, *J* = 8.6, 1.9 Hz, 1H, H-7), 7.29 (d, *J* = 8.4 Hz, 1H, H-8), 5.95 (s, 1H, H-3), 4.85 (dd, *J* = 8.1, 3.7 Hz, 2H, $\mathrm{C\underline{H}_2}$), 4.72 – 4.59 (m, 2H, $\mathrm{C\underline{H}_2}$), 2.20 (s, 3H, $\mathrm{C\underline{H}_3}$); ^{13}C NMR (151 MHz, DMSO) δ 196.52, 196.22, 186.89, 164.51, 161.64, 161.07, 153.32, 151.93, 150.90, 140.63, 133.59, 133.35, 129.14, 128.98, 122.48, 116.20, 114.66, 90.98, 73.31, 67.12, 20.18; IR (ATR) /cm^{-1}: 3077, 2958, 2023 (M–C≡O sym. stretch), 1912 (M–C≡O asym. stretch), 1717, 1575, 1391, 1356, 1275, 1255, 1175, 1131, 1087, 979, 946, 829, 737, 620; Calc. for $C_{21}H_{16}ClN_2O_7Re$ (Mr = 630.0) C, 40.04; H, 2.56; Cl, 5.63; N, 4.45; Re, 29.56; Found:C, 40.10; H, 2.61; Cl, 5.67; N, 4.49; Re, 29.48%.

2.5. *X-Ray crystallography*

The X-ray intensity data for **5d$_{\mathbf{Re}}$**, **6a$_{\mathbf{Re}}$** and **6c$_{\mathbf{Re}}$** were collected on XtaLAB Synergy (Dualflex) CCD diffractometer using monochromatic Cu-Kα (λ = 1.54184 Å) radiation at room temperature. Basic experimental data are given in Table S1. The data were processed with the CrysAlisPro program [69], used for unit cell determination and data reduction. Structures were solved by direct methods using the SHELXT program [70] and refined against F^2 on all data by a full-matrix least squares procedure with the SHELXL program [71]. All non-hydrogen atoms were refined in an anisotropic model of atomic displacement parameters (ADPs). In the structure of **5d$_{\mathbf{Re}}$** two Re complexes with identical chemical composition and different conformation form the asymmetric unit of the structure. Few carbonyl groups coordinated to Re atoms have unusually small C=O bond (C3=O3 bond in one complex), so the distance restraints to the value of 1.2 Å were applied to these bonds, as well as the similar ADPs restraints for atoms in these bonds. Difference electron density in the vicinity of one -CF_3 group in one complex suggest an orientation disordered type, so the final refinement model used the constraint that the sum of occupations for individual orientation is full (1), but each orientation occupation is refined to the values of 0.707(13) and 0.293(13), respectively. Restraint that ADPs for these disorderly oriented F atoms have more isotropic character is also used. Structures **6a$_{\mathbf{Re}}$** and **6c$_{\mathbf{Re}}$** contained only one complex molecule in asymmetric unit of the structure. In both structures, highest difference electron density peaks are located around Re atoms, although for structure **6c$_{\mathbf{Re}}$** these peaks are significant, suggesting higher disorder of the Re atoms. Namely, it is common feature of the structures with Rhenium that significant peaks of difference electron density peaks are located in the vicinity of Re atoms, sometimes these peaks are treated as additional disordered positions of the Re atoms and their occupancies are refined [62,72], however such treatment does not improve significantly the structural model of the complex, especially for the highest occupied position of the Re atom. Positions of hydrogen atoms were treated in the riding model, i.e. they were calculated according to the positions of the carbon atoms to which they are bonded. C-H distances for aromatic, methylene and methyl H-atoms were constrained to 0.93, 0.97 and 0.96 Å, respectively, with isotropic ADP parameter $U_{iso}(H)=1.2xU_{iso}(C)$ for aromatic and methylene H-atoms and $U_{iso}(H)=1.5xU_{iso}(C)$ for methyl H-atoms. Torsion angles of the methyl groups were refined. The CCDC 2370977-2370979 contain the supplementary crystallographic data for this paper.

2.6. Evaluation of the antiproliferative activity

2.6.1. Cell lines and cell culturing

The impact of new synthesized compounds was tested on on human tumor cell lines, including T-lymphoblasts (acute lymphoblastic leukemia) (CCRF-CEM), monocytic (acute monocytic leukemia) (THP1), cervical adenocarcinoma (HeLa), colon adenocarcinoma (CaCo-2), T-cell lymphoma (HuT78), and non-tumor human fibroblasts (BJ).

The cells were cultured in two different types of media: DMEM and RPMI 1640. Both media were supplemented with 2 mM glutamine, fetal bovine serum (10% inactivated by heat), and antibiotics (100 U of penicillin and 0.1mg of streptomycin). The RPMI 1640 was further supplemented with 10 mM HEPES and 1 mM sodium pyruvate. The cells growing in a monolayer were cultured in the DMEM, while the cells growing in suspension were cultured in the RPMI 1640. The cells were grown in a CO_2 incubator (IGO 150 CELLlife^{TM}, JOUAN) under 37 °C in a humidified atmosphere with 5 % CO_2.

2.6.2. Proliferation assay

Growth-inhibitory activity was evaluated using a slightly modified procedure based on the National Cancer Institute's protocol [73]. In brief, the cells were seeded in 96-well microtiter plates and incubated for 24 hours, and then were treated for an additional 72 hours with 10^{-7} to 10^{-4} M concentrations of tested compounds. After treatment period, effects of tested compounds on the cell growth rate were evaluated using the MTT assay [74]. The absorbance was measured at 595 nm with a microplate reader. The IC_{50} values, which represent a 50% inhibition of cell growth, and QC calculation were carried out using the GraphPadPrism and Excel software. The effect of single concentrations was analysed by charting the logarithm of the evaluated compound's concentration against its corresponding percent inhibition value using the least squares fit.

2.7. Cell cycle analysis

The HuT78 cells were plated in 24-well plates at a concentration of 1 x 10^5 cells per well and treated for 24 hours with the selected compounds **5e** and **6d** at a concentration of 50 μM), **5e$_{\mathbf{Re}}$** at a concentration of 10 μM and **6d$_{\mathbf{Re}}$** at a concentration of 2 μM. After drug treatment, the cells were fixed with ice-cold 70 % ethanol in phosphate-buffered saline (PBS) and incubated with 0.3 μg/mL propidium iodide for 30 minutes at room temperature. Prior to analysis by flow cytometry (BD FACSLyric, Becton Dickinson, San Jose, CA, SAD), samples were treated with 0.4 μg/mL RNase A for 5 minutes at room temperature. The resulting DNA histograms were generated and analysed using FlowJo 10.10. software (Treestar, Inc, Ashland, OR, USA).

2.8. Measurement of mitochondrial membrane potential (ΔΨm)

The changes in (ΔΨm) were measured with the dye 75 nM TMRE (tetramethylrhodamine, ethyl ester, perchlorate). In brief, the tested cells (HuT78) were plated in 96-well plates at a concentration of 1.5 x 10^5 cells per well and treated with 50 μM **5e** and **6d**, 10 μM **$5e_{Re}$** and 2 μM **$6d_{Re}$**. After 24 hours of treatment, cells were harvested, centrifuged at 1100 rpm for 6 minutes and stained with 200 nM TMRE dye according to the kit protocol (TMRE Mitochondrial Membrane Potential Assay Kit, abcam, UK). Positive control cells were treated with 20 μM FCCP (carbonyl cyanide-p-trifluoromethoxyphenylhydrazone) for 10 minutes. Cells were analysed with multimode microplate reader Tecan Spark (Tecan, Mannedorf, Switzerland) fusing fluorescence filter setting (Ex/Em = 490/595 nm) and the Sparkcontrol method editor software.

2.9. Determination of intracellular free oxygen radicals (ROS) and superoxide production

HuT78 cells were resuspended at a concentration of 1 x 10^5 cells/mL in PBS and incubated for 1 hour in an incubator at 37 °C/5 % CO_2 with with 50 μM **5e** and **6d**, 10 μM **$5e_{Re}$** and 2 μM **$6d_{Re}$**. At the end of the incubation period, reagents were added to the cells according to the manufacturer's instructions from the Fluorometric Intracellular Ros Kit (Sigma-Aldrich, St. Louis, USA) and the cells were then incubated in an incubator at 37 °C/5 % CO_2 for 30 minutes. Cell analysis was performed with Tecan Spark Multimode Microplate Reader (Tecan, Mannedorf, Switzerland) using the Sparkcontrol Method Editor software. Intracellular free oxygen radicals are detected with a green fluorescence filter setting (Ex/Em = 490/595 nm), while superoxide production was detected by an orange fluorescence signal (Ex/Em = 550/620 nm). Experiments were performed in triplicate and quantitative data are expressed as mean ± standard deviation. STATISTICA 14.0.1.8. (TIBCO Software Inc., Tulsa, USA) was used to statistically analyse the results. Student’s t-test was used to analyse the data. A P-value of less than 0.05 was considered statistically significant.

3. Results and discussion

3.1. *Chemistry and spectroscopic characterization*

Novel quinoline and coumarin ligands were synthesized as shown in Scheme 1. First, 2-(trifluoromethyl)quinolin-4-ol derivatives substituted at C-6 position were obtained by a Knoevenagel condensation of various *p*-substituted aniline derivatives and ethyl 4,4,4-trifluoroacetoactate in the presence of polyphosphoric acid (PPA) at 150 °C (Scheme S1, Supplementary Material). *O*-Alkylated (*E*)-picolinaldehyde oxime **2** was synthesized by base-promoted alkylation of *syn*-2-pyridinealdoxime with 1,2-dibromoethane. Finally, reaction of corresponding quinoline **3a–3e** or coumarin **4a–4d** and *O*-alkylated (*E*)-picolinaldehyde oxime **2** with NaH afforded targeted quinoline **5a–5e** and coumarin **6a–6d** ligands in moderate yield (41–81%).

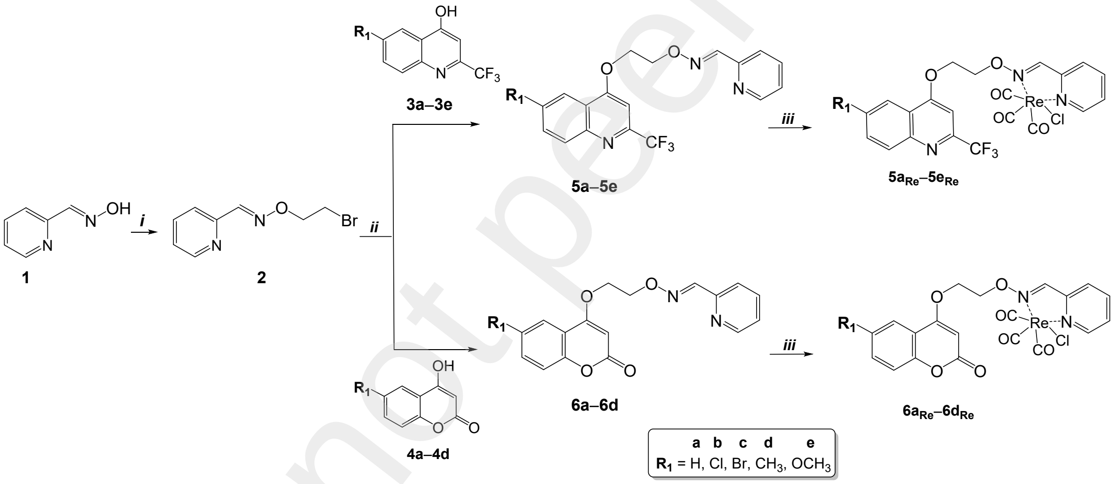

Scheme 1. Synthesis of quinoline and coumarin derivatives with aldoxime-ether linked pyridine moieties and corresponding $Re[(CO)_3]^+$ metal complexes. *Reagents and conditions:* (*i*) 1,1-dibromoethane, NaH, DMF, r.t, 24 h; (*ii*) K_2CO_3, DMF, 80 °C, 24 h (*iii*) $[Re(CO)_5Cl]$, $CHCl_3$, reflux, 24 h.

Ligands **5a–5e** and **6a–6d** subsequently reacted with $[Re(CO)_5Cl]$ to obtain the corresponding rhenium(I) tricarbonyl complexes **5a$_{Re}$–5e$_{Re}$** and **6a$_{Re}$–6d$_{Re}$** in good yield (40–89%). Ligands and complexes were fully characterized by ^1H and ^{13}C NMR, as well as IR and UV-Vis spectroscopy (Figures S7-S83, Table S3, Supplementary Material). The purity of both the ligands and the complexes was confirmed by elemental analysis. The difference between the ^1H NMR spectra of the ligands and their rhenium(I) tricarbonyl complexes is the deshielding of pyridine, aldoxime and methylene protons due to the electron-withdrawing inductive effects of the transition metal. Significant shifts are observed for the aldoxime proton and the pyridine proton in *ortho* position to the *N*-donor atom. Both the aldoxime protons ($\Delta\delta \approx 1.2$ ppm) and pyridine protons ($\Delta\delta \approx 0.4$ ppm) experience strong deshielding effects, which are observed in both coumarin and quinoline complexes. Fig. 3 illustrates the observed trends of the chemical shift in the coordination of **6c** with the Re(I) ion. The ^{13}C NMR spectra of the metal complexes show three signals in the range of 197–189 ppm, which correspond to the carbon atoms of the carbonyl group and indicate the presence of [Re(CO)$_3$Cl] in the structures of the metal complexes. IR spectroscopy further confirmed the complexation due to the appearance of strong ν(CO) symmetric and asymmetric stretching modes expected for *fac*-[Re(CO)$_3$Cl] groups in the range of 2026–1884 cm^{-1} (Figures S48-S74, Table S3, Supplementary Material).

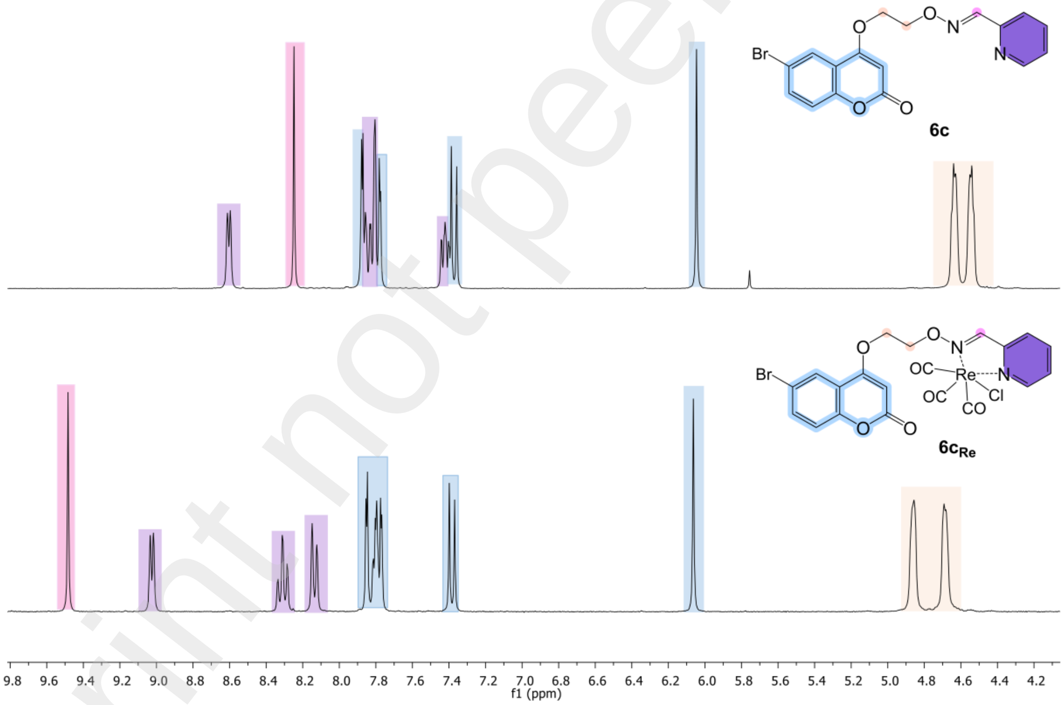

Fig. 3. Comparison of the proton NMR spectra of ligand **6c** and rhenium(I) tricarbonyl complex **6c$_{\mathbf{Re}}$** in DMSO-d_6.

3.2. *Solid state characterization*

The crystals of the quinoline complex **$5d_{Re}$** and the coumarin complexes **$6a_{Re}$** and **$6c_{Re}$** were obtained by slow evaporation from dichloromethane : methanol solutions. The structures are shown in Fig. 4, while the parameters of crystallographic refinement and data acquisition as well as the relevant interatomic distances and angles are listed in Tables S1 and S2. In all complexes, the ligands coordinate with the metal ion in a bidentate manner, resulting in an octahedral geometry with an N_2C_3Cl coordination sphere around Re(I). The crystal structures of the complexes show the expected *fac*-stereochemistry, which is due to the influence of back-bonding of the CO ligands. In all complexes, the metal centre is coordinated by $N_{pyridine}$ and $N_{aldoxime}$, with the chloride ion in these complexes is covalently bonded to the metal. The bond lengths and bond angles observed in all complexes are consistent with the typical structural features identified in previous studies of rhenium tricarbonyl complexes with bidentate ligands (*fac*-[Re(X)(CO)$_3$(N^N)]) [75–78]. For example, the average length of the Re-carbonyl bond is 1.94(4) Å, with the OC–Re–CO angles forming an almost regular trigonal pyramid with angles between 87.3(3) and 92.1(3) degrees. In addition, the average lengths of the Re–Cl bonds are between 2.430(2) and 2.470(2) Å.

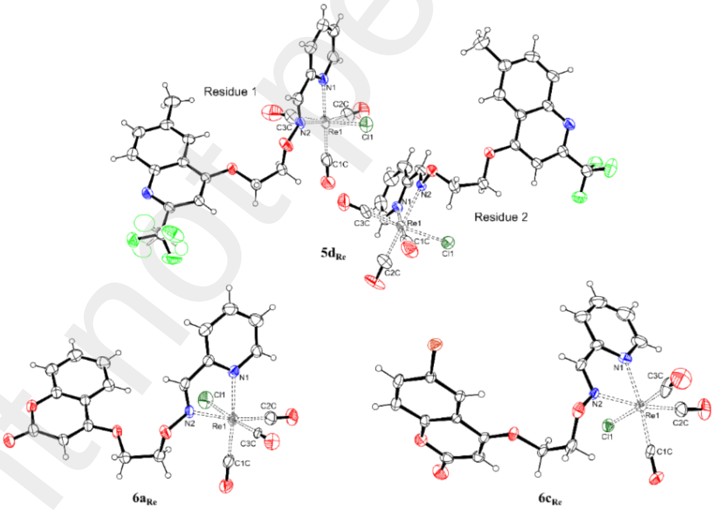

Fig. 4. Crystal structure of the complexes **$5d_{Re}$**, **$6a_{Re}$** and **$6c_{Re}$**. Only metal and coordinating atoms are labelled. The comprehensive labelling schemes are shown in Figures S1, S2, and S3 (Supplementary Material).

3.3. Biological evaluation

3.3.1. Antiproliferative evaluation

The results of antiproliferative evaluation of novel quinoline and coumarin ligands **5a**–**5e** and **6a**–**6f** and their rhenium(I) tricarbonyl complexes **5a**$_{\text{Re}}$–**5e**$_{\text{Re}}$ and **6a**$_{\text{Re}}$–**6d**$_{\text{Re}}$ on human tumor cell lines, including T-lymphoblasts (acute lymphoblastic leukemia) (CCRF-CEM), monocytic (acute monocytic leukemia) (THP1), cervical adenocarcinoma (HeLa), colon adenocarcinoma (CaCo-2), T-cell lymphoma (HuT78), and non-tumor human fibroblasts (BJ) are presented in Table 1. 5-Fluorouracil (5-FU) is included as a reference drug.

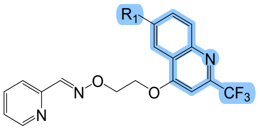

5a–5e

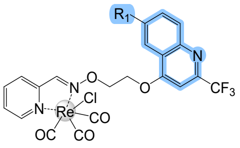

5a$_{\text{Re}}$**–5e**$_{\text{Re}}$

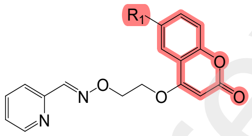

6a–6d

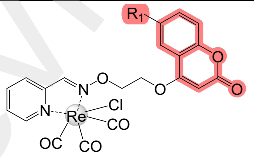

6a$_{\text{Re}}$**–6d**$_{\text{Re}}$

		IC$_{50}$^{a} (µM)						SI (HuT78)^{b}
R1	Compd	**CCRF-CEM**	**HeLa**	**CaCo-2**	**THP-1**	**HuT78**	**BJ**	
H	**5a**	94.9±40	>100	>100	86.4 ± 11.4	43.4±1.6	>100	2.3
	5a$_{\text{Re}}$	11.5±7.9	20.2±1.2	28.4±2.4	16.1±0.7	29.0±1.6	64.0±3.4	2.2
Cl	**5b**	>100	>100	>100	64.6±5.9	24.9±0.2	>100	4.1
	5b$_{\text{Re}}$	22.1±1.1	20.7±0.7	28.9±5.6	26.7±8.7	10.4±0.2	30.1±2.3	2.9
Br	**5c**	42.1±0.9	>100	>100	49.1±11.4	33.2±5.9	>100	4.3
	5c$_{\text{Re}}$	6.3±1.7	21.8±1.5	30.6±1.5	10.6±1.7	11.0±1.2	21.0±5.2	1.9
CH$_3$	**5d**	81.1±11.0	>100	<100	55.2±7.01	41.2±1.7	>100	2.4
	5d$_{\text{Re}}$	15.9±2.2	39.3±20.9	56.4±25.1	17.8±3.0	10.2±2.3	31.5±6.2	3.1
OCH$_3$	**5e**	>100	>100	>100	76.4±7.5	48.7±3.3	>100	2.1
	5e$_{\text{Re}}$	17.2±6.6	27.9±11.7	29.4±7.4	36.1±3.7	**9.4±0.1**	**54.5±2.7**	**5.8**
H	**6a**	46.5±7.1	>100	>100	46.2±5.1	49.2±5.5	>100	2.2
	6a$_{\text{Re}}$	26.0±10.5	>100	>100	71.0±5.7	40.5±7.1	>100	2.5
Cl	**6b**	89.5±33.4	>100	>100	56.2±5.9	44.8±37.3	>100	2.2
	6b$_{\text{Re}}$	24.4±0.8	>100	>100	25.8±1.6	34.9±1.4	78.1±2.5	2.2
Br	**6c**	94.0±11.1	>100	>100	39.6±7.2	44.7±0.3	>100	2.3
	6c$_{\text{Re}}$	9.5±2.7	19.1±2.3	33.2±6.2	15.4±2.1	10.6±1.0	59.1±5.9	5.6
CH$_3$	**6d**	78.2±19.7	>100	>100	37.9±8.2	43.8±5.4	>100	2.3
	6d$_{\text{Re}}$	13.0±2.9	22.5±0.7	32.0±3.0	16.5±1.9	**2.4±0.8**	**20.9±1.8**	**8.7**
	5Fu	52.2±0.8	8.2±1.9	5.9±0.7	76.4±0.5	>100	16.8 ± 7.0	/

[a] 50% inhibitory concentration or compound concentration required to inhibit tumor cell proliferation by 50%. [b] SI, selectivity index, SI = IC$_{50}$ for normal cell line/IC$_{50}$ for cancer cell line (HuT78).

Table 1. The growth–inhibition effects *in vitro* of compounds **5a–e** and **6a–f** and their rhenium(I) tricarbonyl complexes **5a**$_{\text{Re}}$**–5e**$_{\text{Re}}$ and **6a**$_{\text{Re}}$**–6d**$_{\text{Re}}$ on selected tumor cell lines.

A comparison of the antiproliferative activity of quinoline and coumarin derivatives with pyridine aldoxime moiety showed that quinolines **5a**–**5e** have a higher activity than corresponding coumarins **6a**–**6d**. As shown in Table 1, 6-chloro-2-(trifluoromethyl)quinoline ligand **5b** and 6-bromo-2-(trifluoromethyl)quinoline ligand **5c** showed a good (**5b**: IC_{50} = 24.9 μM, **5c**: IC_{50} = 33.2 μM) and selective inhibitory activity on T-cell lymphoma (HuT78). Compounds were non-toxic ($IC_{50} > 100$ μM) to non-tumor human fibroblasts (BJ). 6-Methyl-2-(trifluoromethyl)quinoline **5d** and 6-methoxy-2-(trifluoromethyl)quinoline **5e** ligands showed slightly less activity (**5d**: IC_{50} = 41.2 μM; **5e**: IC_{50} = 48.7 μM) on HuT78 cells relative to **5b** and **5c**. Among the coumarin ligands, all tested compounds (**6a–6d**) exhibited moderate inhibitory activity on HuT78 cells with IC_{50} values ranging from 43.8 to 49.2 μM.

Rhenium(I) tricarbonyl complexes of both quinolines **5a$_{Re}$**–**5e$_{Re}$** and coumarins **6a$_{Re}$**–**6d$_{Re}$** exhibited better growth-inhibitory effect on cancer cell lines than their ligands (Figure 5). Thus, antiproliferative activity of quinoline-based complexes **5a$_{Re}$**–**5e$_{Re}$** on HuT78 cells increased from 2-fold to 5-fold relative to corresponding ligands **5a**–**5e**. However, some rhenium organometallic complexes were also cytotoxic to non-tumor BJ cells. Their cytotoxicity was comparable or lower than that of 5-FU. In the group of quinoline-based complexes, 6-methoxy-2-(trifluoromethyl)quinoline complex **5e$_{Re}$** showed the best activity (IC_{50} = 9.4 μM) and selectivity (SI = 5.8) on HuT78 cells. 6-Unsubstituted 2-(trifluoromethyl)quinoline **5a$_{Re}$** showed moderate activity on all evaluated cell lines with IC_{50} values in the range from 11.5 to 29 μM.

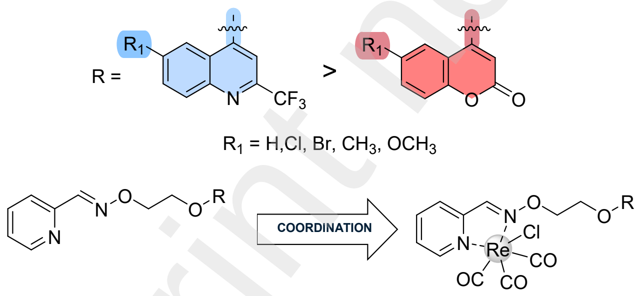

➡ quinoline derivatives are more active than coumarin derivatives

➡ antitumor activity of quinoline ligands decreases in the order: Cl > CH_3 > H > Br > OCH_3

➡ antitumor activity of comarin ligands decreases in the order: CH_3 > Br > H > Cl

➡ $[Re(CO)_3]^+$ fragment enhances anticancer activity but reduces selectivity

Fig. 5. Insight into structure-activity relationship of the ligands **5a**–**5e** and **6a**–**6d** and their Re(I) complexes on antiproliferative activity.

Among the coumarin-based complexes, 6-methylcoumarin complex **6d$_{Re}$** showed a marked and selective antiproliferative effect (IC_{50} = 2.4 μM, SI = 8.7) on HuT78 cells. Both the bromo-substituted quinoline **5c$_{Re}$** and coumarin **6c$_{Re}$** complexes showed an inhibitory activity on T-lymphoblasts (CCRF-CEM) (**5c$_{Re}$**: IC_{50} = 6.3 μM; **6c$_{Re}$**: IC_{50} = 9.5 μM) and monocytic leukemia (THP1) (**5c$_{Re}$**: IC_{50} = 10.6 μM; **6c$_{Re}$**: IC_{50} = 15.4 μM) and moderate activity on cervical adenocarcinoma (HeLa) and colon adenocarcinoma (CaCo-2). Their activities were greater than those of 5-FU, with the exception of inhibition of HeLa and CaCo-2 cells. The metal coordination of quinoline increased the activity of complex **5c$_{Re}$** over ligand **5c** on CCRF-CEM cells by 7-fold. The 6-chloro-2-(trifluoromethyl)quinilone complex **5b$_{Re}$** was also 5-fold more active (IC_{50} = 2.7 μM) than its ligand **5b** (Table 1). The observed results of pronounced antiproliferative activity of the metal complexes compared to their coumarin and quinoline ligands are in agreement with the results of previously published studies [79–81]. Based on the results of antiproliferative activity and selectivity, four compounds (**5e**, **5e$_{Re}$**, **6d** and **6d$_{Re}$**were chosen for further biological evaluations) as representatives of quinolones and coumarins.

3.3.2. Cell cycle modification

One of the possible mechanisms involved in the treatment of cancer is the interruption of the cell cycle [49,82]. The cell cycle distribution in HuT78 cells was analysed to determine whether ligands **5e** and **6d** and their complexes **5e$_{Re}$** and **6d$_{Re}$** inhibit the proliferation of these cells by cell cycle arrest. These compounds were selected because the metal complex **5e$_{Re}$** showed the most pronounced and most selective inhibitory effect in the group of quinoline derivatives, and the metal complex **6d$_{Re}$** showed the strongest and most selective inhibition of HuT78 cell growth among the coumarin derivatives compared to their effect on the growth of non-tumor BJ cells. HuT78 cells were exposed to the compounds for 24 hours at the concentration required to inhibit tumour cell proliferation by 50% (IC_{50}). As shown in Fig. 6, all tested compounds caused a significant accumulation of cells in the G0/G1 phase of the cell cycle and a significant decrease in the number of cells in the G2/M phase of the cell cycle. The population of HuT78 cells in the G0/G1 phase increased from 30.9 % (control group) to 60.5 % (**5e**), 50.1 % (**5e$_{Re}$**), 57.1 % (**6d)** and 47.3 % (**6d$_{Re}$**), while the percentage of cells in the G2/M phase decreased significantly compared to the non-treated cells (Fig. 6). These compounds affect the same phases of the cell cycle and lead to changes in cell proliferation and growth. The ability of tricarbonyl rhenium complexes to stop the passage of cells in the M/G2 phase of the cell cycle was also observed in the study by Simpson et al. [83]. Numerous studies have shown that quinoline- and coumarin-based compounds and their hybrids significantly affect the growth of tumor cells in different phases of the cell cycle, most frequently in the G0/G1 phase [84–86]. These data suggest that the observed cell cycle arrest contributes to the proliferation inhibitory effects of the tested compounds on HuT78 cells.

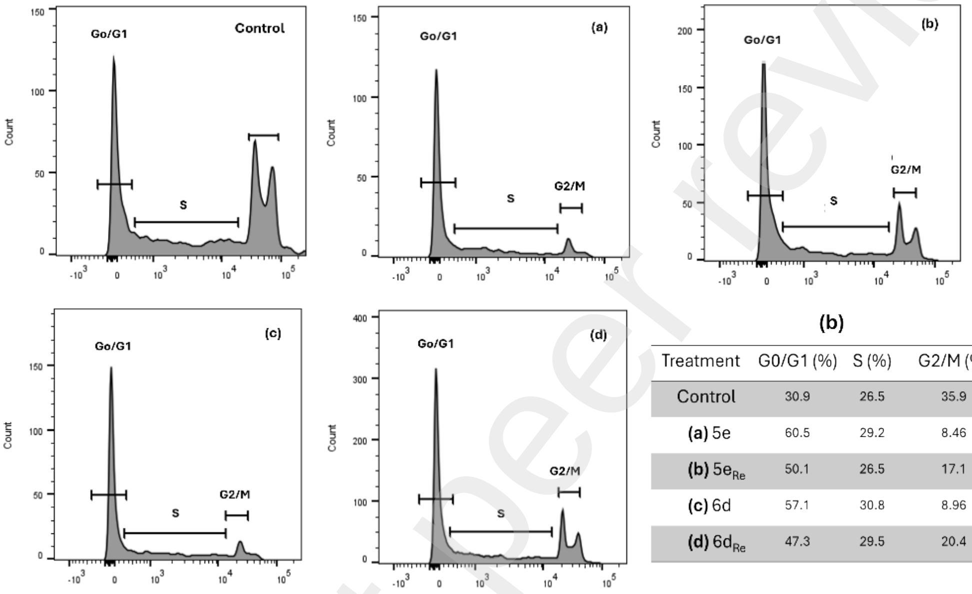

(b)

Treatment	G0/G1 (%)	S (%)	G2/M (%)
Control	30.9	26.5	35.9
(a) 5e	60.5	29.2	8.46
(b) $5e_{Re}$	50.1	26.5	17.1
(c) 6d	57.1	30.8	8.96
(d) $6d_{Re}$	47.3	29.5	20.4

Fig. 6. Flow cytometric analysis of the cell cycle distribution of HuT78 cells exposed to compounds **5e** and **6d** (50 µM), **$5e_{Re}$** (10 µM), and **$6d_{Re}$** (2 µmol dm^{-3}) for 24 hours. (**a**) DNA histograms show changes in the cell cycle. (**b**) Data are presented as percentage (%) of cells in the cell cycle phase.

3.3.3. Reactive oxygen species ROS production in treated tumor cells

Tumor cells contain higher concentrations of ROS than normal cells, but when intracellular ROS concentrations increase drastically to toxic levels, oxidative stress causes irreversible damage and can eventually lead to cancer cell death [87,88]. ROS can be generated by various cellular processes or chemical reactions [89]. The most important ROS for physiological and cancer processes are singlet oxygen, superoxide anions, hydroxyl radicals and hydrogen peroxide [88].

Total ROS and superoxide production in HuT78 cells were investigated to better understand the observed cytotoxic and cell cycle effects of the novel quinoline (**5e**) and coumarin (**6d**) ligands and their complexes with rhenium(I) (**5e**$_{\mathbf{Re}}$ and **6d**$_{\mathbf{Re}}$) (Fig. 7). Our aim was to determine whether our novel quinoline and coumarin metal complexes behave as ROS generators in tumor cells, as shown in recently published studies [88,90,91], or whether they have no effect on ROS production, as suggested by the results of the study by Sharma et al. [92].

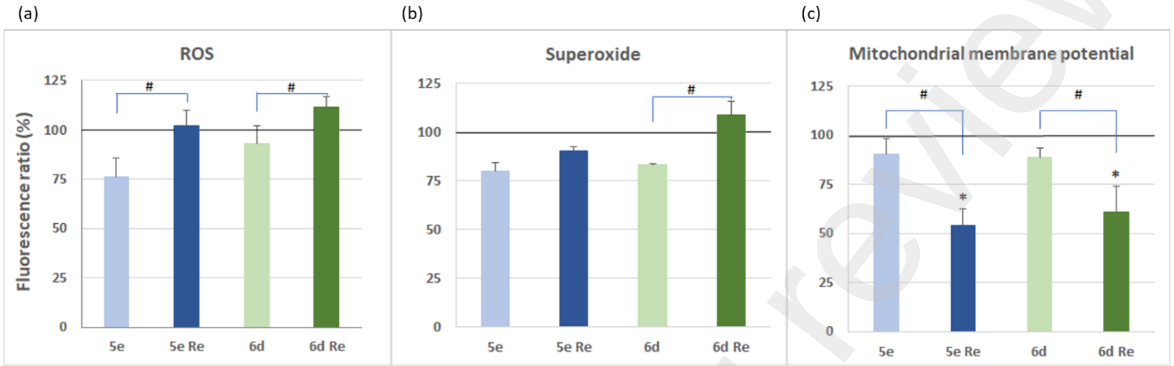

Fig. 7. Evaluation of changes in: a) ROS production; b) superoxide production and c) mitohondrial membrane potential after exposure of HuT78 cells to **5e**, **6d** (50 µM), **5e**$_{\mathbf{Re}}$ (10 µM) and **6d**$_{\mathbf{Re}}$ (2 µM) for 24 hours. Data are presented as mean and standard deviation of three independent measurements in triplicate. A statistically significant p value is defined as $p < 0.05$ (*, $^{\#}$).

As can be seen in Fig. 7a, complexes **5e**$_{\mathbf{Re}}$ and **6d**$_{\mathbf{Re}}$ slightly, but not significantly, increased the production of total ROS, while compounds **5e** and **6d** slightly decreased the production of total ROS compared to ROS production in untreated HuT78 cells. The difference in the effect of compounds **5e** and **6d** compared to their rhenium(I) complexes is that **5e** and **6d** significantly reduced the production of ROS. Since the formation of superoxide radicals is a consequence of the incomplete redox reaction of oxygen molecules or during the production of adenosine triphosphate, we measured them separately. Compounds **5e**, **6d** and **5e**$_{\mathbf{Re}}$ slightly decreased the synthesis of superoxide anions, while compound **6d**$_{\mathbf{Re}}$ increased their concentration by about 20 % compared to non-treated (control) cells (Fig. 7b). Although an increase in superoxide and other reactive oxygen species was expected when tumor cell lines were treated with antitumor agents, a reduction in their levels may mean that the pathway for ROS production in the cells is inhibited and the processes necessary for cell survival are disrupted.

The overproduction of ROS in the mitochondria occurs in tumor cells due to an increased metabolic rate, a gene mutation and relative hypoxia. Cytotoxic compounds often reduce mitochondrial membrane potential [93,94]. A decrease in mitochondrial membrane potential can increase ROS production and trigger treated cell death [94,95]. As shown in Fig. 7c, compounds **5e** and **6d** showed no significant effect on mitochondrial membrane potential. Their rhenium(I) tricarbonyl complexes reduced the mitochondrial membrane potential by 50% (**5e$_{\mathbf{Re}}$**) and by 45% (**6d$_{\mathbf{Re}}$**) compared to untreated cells and compared to cells treated with **5e** and **6d**, respectively. These results suggest that the cytotoxic effects of these compounds are mediated, at least in part, by their effects on mitochondrial membrane potential and the subsequent increase in ROS production. Understanding these mechanisms is critical for the development of effective cancer therapies that target mitochondrial function and oxidative stress pathways.

4. Conclusions

Quinolines, obtained by Knoevenagel condensation, and coumarins were synthesized by base-promoted *O*-alkylation with (*E*)-picolinaldehyde oxime to afford quinolines **5a–5e** and coumarins **6a–6d** with aldoxime ether linked pyridine moiety. Quinoline and coumarin ligands subsequently reacted with [Re(CO)$_5$Cl] to obtain the corresponding rhenium(I) tricarbonyl complexes **5a$_{\mathbf{Re}}$–5e$_{\mathbf{Re}}$** and **6a$_{\mathbf{Re}}$– 6d$_{\mathbf{Re}}$**.

The results of the antiproliferative evaluations showed that Re(I) coordination of quinoline and coumarin ligands enhanced the activity of these complexes up to 18-fold compared to the corresponding ligands alone. Notably, quinoline complexes **5a$_{\mathbf{Re}}$–5e$_{\mathbf{Re}}$** were more active than coumarin complexes **6a$_{\mathbf{Re}}$–6d$_{\mathbf{Re}}$**, showing pronounced activity against T-cell lymphoma (HuT78). Among the quinoline rhenium-complexes, 6-methoxy-2-(trifluoromethyl)quinoline complex **5e$_{\mathbf{Re}}$** showed the best growth-inhibition effect on HuT78 cells (IC$_{50}$ = 9.4 μM) with a selectivity index of 5.8. Within the group of coumarin rhenium(I) tricarbonyl complexes, **6d$_{\mathbf{Re}}$** showed the most significant effect on the growth of HuT78 cells with an IC$_{50}$ of 2.4 μM and a selectivity index of 8.7.

Ligands **5e** and **6d** and their complexes **5e$_{\mathbf{Re}}$**, and **6d$_{\mathbf{Re}}$** were found to arrest the cell cycle of HuT78 cells, causing a significant accumulation of cells in the G0/G1 phase and a marked decrease in the number of cells in the G2/M phase. The rhenium(I) tricarbonyl complexes slightly increased ROS production and significantly reduced mitochondrial membrane potential by 50% (**5e$_{\mathbf{Re}}$**) and by 45% (**6d$_{\mathbf{Re}}$**) compared to untreated cells and cells treated with **5e** and **6d**. These results suggest that the cytotoxic effects of these compounds are mediated, at least in part, by their effects on mitochondrial membrane potential and the subsequent increase in ROS production. Further chemical and pharmacological optimization is warranted to obtain structurally related quinoline- and coumarin-based lead compounds as pronounced and selective agents for T-cell lymphoma.

CRediT authorship contribution statement

Martina Piškor: Writing – original draft, Formal analysis, Methodology; Ivan Ćorić: Investigation, Formal analysis; Berislav Perić: Writing – original draft, Formal analysis, Methodology; Katarina Mišković Špoljarić: Investigation, Formal analysis; Srećko I. Kirin: Writing – original draft, review and editing; Ljubica Glavaš-Obrovac: Writing – original draft, review and editing, Supervision; Silvana Raić-Malić: Writing – original draft, review and editing, Supervision, Project administration.

Declaration of competing interest

The authors declare no conflict of interest.

Data availability

Data will be made available on request.

Acknowledgement

We greatly appreciate the financial support of the Croatian Science Foundation (project No. IP-2022-10-9420).

Appendix A. Supplementary data

Supplementary data to this article can be found online at https://doi...

References

[1] F. Bray, M. Laversanne, H. Sung, J. Ferlay, R.L. Siegel, I. Soerjomataram, A. Jemal, Global cancer statistics 2022: GLOBOCAN estimates of incidence and mortality worldwide for 36 cancers in 185 countries, CA. Cancer J. Clin. 74 (2024) 229–263. https://doi.org/10.3322/caac.21834.

[2] Global cancer burden growing, amidst mounting need for services, (n.d.). https://www.who.int/news/item/01-02-2024-global-cancer-burden-growing--amidst-mounting-need-for-services.

[3] H. Tsuda, K. Takatsuki, R. Ohno, T. Masaoka, K. Okada, S. Shirakawa, Y. Ohashi, K. Ota, Treatment of adult T-cell leukaemia-lymphoma with irinotecan hydrochloride (CPT-11), Br. J. Cancer. 70 (1994) 771–774. https://doi.org/10.1038/bjc.1994.394.

[4] K.O. Alfarouk, C.M. Stock, S. Taylor, M. Walsh, A.K. Muddathir, D. Verduzco, A.H.H. Bashir, O.Y. Mohammed, G.O. Elhassan, S. Harguindey, S.J. Reshkin, M.E. Ibrahim, C. Rauch, Resistance to cancer chemotherapy: Failure in drug response from ADME to P-gp, Cancer Cell Int. 15 (2015) 1–13. https://doi.org/10.1186/s12935-015-0221-1.

[5] A. Ramos, S. Sadeghi, H. Tabatabaeian, Battling chemoresistance in cancer: Root causes and strategies to uproot them, Int. J. Mol. Sci. 22 (2021) 1–22. https://doi.org/10.3390/ijms22179451.

[6] M. Ilakiyalakshmi, A. Arumugam Napoleon, Review on recent development of quinoline for anticancer activities, Arab. J. Chem. 15 (2022) 104168. https://doi.org/10.1016/j.arabjc.2022.104168.

[7] O. Afzal, S. Kumar, M.R. Haider, M.R. Ali, R. Kumar, M. Jaggi, S. Bawa, A review on anticancer potential of bioactive heterocycle quinoline, Eur. J. Med. Chem. 97 (2015) 871–910. https://doi.org/10.1016/j.ejmech.2014.07.044.

[8] M. Koley, J. Han, V.A. Soloshonok, S. Mojumder, R. Javahershenas, A. Makarem, Latest developments in coumarin-based anticancer agents: Mechanism of action and structure-activity relationship studies, RSC Med. Chem. 15 (2024) 10–54. https://doi.org/10.1039/d3md00511a.

[9] L. Pisani, M. Catto, G. Muncipinto, O. Nicolotti, A. Carrieri, M. Rullo, A. Stefanachi, F. Leonetti, C. Altomare, A twenty-year journey exploring coumarin-based derivatives as bioactive molecules, Front. Chem. 10 (2022) 1–8. https://doi.org/10.3389/fchem.2022.1002547.

[10] L. Zhang, Z. Xu, Coumarin-containing hybrids and their anticancer activities, Eur. J. Med. Chem. 181 (2019) 111587. https://doi.org/10.1016/j.ejmech.2019.111587.

[11] L.F.E. Moor, T.R.A. Vasconcelos, R. da R. Reis, L.S.S. Pinto, T.M. da Costa, Quinoline: An attractive scaffold in drug design, Mini-Reviews Med. Chem. 21 (2021) 2209–2226. https://doi.org/10.2174/1389557521666210210155908.

[12] S. Jain, V. Chandra, P. Kumar Jain, K. Pathak, D. Pathak, A. Vaidya, Comprehensive review on current developments of quinoline-based anticancer agents, Arab. J. Chem. 12 (2019) 4920–4946. https://doi.org/10.1016/j.arabjc.2016.10.009.

[13] X.F. Song, J. Fan, L. Liu, X.F. Liu, F. Gao, Coumarin derivatives with anticancer activities: An update, Arch. Pharm. (Weinheim). 353 (2020) 1–11. https://doi.org/10.1002/ardp.202000025.

[14] N. Bhattarai, A.A. Kumbhar, Y.R. Pokharel, P.N. Yadav, Anticancer potential of coumarin and its derivatives, Mini Rev. Med. Chem. 21 (2021) 2996–3029. https://doi.org/10.2174/1389557521666210405160323.

[15] A. Ibrar, S.A. Shehzadi, F. Saeed, I. Khan, Developing hybrid molecule therapeutics for diverse enzyme inhibitory action: Active role of coumarin-based structural leads in drug discovery, Bioorg. Med. Chem. 26 (2018) 3731–3762. https://doi.org/10.1016/j.bmc.2018.05.042.

[16] F. Hersi, H.A. Omar, R.A. Al-Qawasmeh, Z. Ahmad, A.M. Jaber, D.M. Zaher, T.H. Al-Tel, Design and synthesis of new energy restriction mimetic agents: Potent anti-tumor activities of hybrid motifs of aminothiazoles and coumarins, Sci. Rep. 10 (2020) 1–17. https://doi.org/10.1038/s41598-020-59685-x.

[17] E.F. Bruna-Haupt, M.D. Perretti, H.A. Garro, R. Carrillo, F. Machín, I. Lorenzo-Castrillejo, L. Gutiérrez, E.G. Vega-Hissi, M. Mamberto, M. Menacho-Marquez, C.O. Fernández, C. García, C.R. Pungitore, Synthesis of structurally related coumarin derivatives as antiproliferative agents, ACS Omega. 8 (2023) 26479–26496. https://doi.org/10.1021/acsomega.3c03181.

[18] D. Cao, Y. Liu, W. Yan, C. Wang, P. Bai, T. Wang, M. Tang, X. Wang, Z. Yang, B. Ma, L. Ma, L. Lei, F. Wang, B. Xu, Y. Zhou, T. Yang, L. Chen, Design, synthesis, and evaluation of in vitro and in vivo anticancer activity of 4-substituted coumarins: a novel class of potent tubulin polymerization inhibitors, J. Med. Chem. 59 (2016) 5721–5739. https://doi.org/10.1021/acs.jmedchem.6b00158.

[19] M. Basanagouda, V.B. Jambagi, N.N. Barigidad, S.S. Laxmeshwar, V. Devaru, Narayanachar, Synthesis, structure-activity relationship of iodinated-4-aryloxymethyl-coumarins as potential anti-cancer and anti-mycobacterial agents, Eur. J. Med. Chem. 74 (2014) 225–233. https://doi.org/10.1016/j.ejmech.2013.12.061.

[20] A. Thakur, R. Singla, V. Jaitak, Coumarins as anticancer agents: A review on synthetic strategies, mechanism of action and SAR studies, Eur. J. Med. Chem. 101 (2015) 476–495. https://doi.org/10.1016/j.ejmech.2015.07.010.

[21] S. Parveen, F. Arjmand, S. Tabassum, Development and future prospects of selective organometallic compounds as anticancer drug candidates exhibiting novel modes of action, Eur. J. Med. Chem. 175 (2019) 269–286. https://doi.org/10.1016/j.ejmech.2019.04.062.

[22] J. Karges, R.W. Stokes, S.M. Cohen, Metal complexes for therapeutic applications, Trends Chem. 3 (2021) 523–534. https://doi.org/10.1016/J.TRECHM.2021.03.006.

[23] K.D. Mjos, C. Orvig, Metallodrugs in medicinal inorganic chemistry, Chem. Rev. 114 (2014) 4540–4563. https://doi.org/10.1021/cr400460s.

[24] P. Chellan, P.J. Sadler, Enhancing the activity of drugs by conjugation to organometallic fragments, Chem. A Eur. J. 26 (2020) 8676–8688.

https://doi.org/10.1002/chem.201904699.

[25] R. Kumar, A. Thakur, Sachin, D. Chandra, A. Kumar Dhiman, P. Kumar Verma, U. Sharma, Quinoline-based metal complexes: Synthesis and applications, Coord. Chem. Rev. 499 (2024) 215453. https://doi.org/https://doi.org/10.1016/j.ccr.2023.215453.

[26] Z.F. Wang, X.L. Nai, Y. Xu, F.H. Pan, F.S. Tang, Q.P. Qin, L. Yang, S.H. Zhang, Cell nucleus localization and high anticancer activity of quinoline-benzopyran rhodium(III) metal complexes as therapeutic and fluorescence imaging agents, Dalton Trans. 51 (2022) 12866–12875. https://doi.org/10.1039/d2dt01929a.

[27] S. Adsule, V. Barve, D. Chen, F. Ahmed, Q.P. Dou, S. Padhye, F.H. Sarkar, Novel Schiff base copper complexes of quinoline-2 carboxaldehyde as proteasome inhibitors in human prostate cancer cells, J. Med. Chem. 49 (2006) 7242–7246. https://doi.org/10.1021/jm060712l.

[28] H. El-Halim, G. Mohamed, M. Anwar, Antimicrobial and anticancer activities of Schiff base ligand and its transition metal mixed ligand complexes with heterocyclic base, Appl. Organomet. Chem. 32 (2017) e3899. https://doi.org/10.1002/aoc.3899.

[29] A.D.M. Mohamad, M.J.A. Abualreish, A.M. Abu-Dief, Antimicrobial and anticancer activities of cobalt (III)-hydrazone complexes: Solubilities and chemical potentials of transfer in different organic co-solvent-water mixtures, J. Mol. Liq. 290 (2019) 111162. https://doi.org/10.1016/j.molliq.2019.111162.

[30] A.A. Adeleke, S.J. Zamisa, M.S. Islam, K. Olofinsan, V.F. Salau, C. Mocktar, B. Omondi, Quinoline functionalized Schiff base silver (I) complexes: Interactions with biomolecules and in vitro cytotoxicity, antioxidant and antimicrobial activities, Molecules 26 (2021) 1205. https://doi.org/10.3390/molecules26051205.

[31] G. Gokulnath, R. Manikandan, P. Anitha, C. Umarani, Synthesis, characterization, in vitro antimicrobial and anticancer activity of metal(II) complexes of Schiff base-derived from 3-formyl-2-mercaptoquinoline and thiosemicarbazide, Phosphorus Sulfur Silicon Relat. Elem. 196 (2021) 1078–1083. https://doi.org/10.1080/10426507.2021.1966630.

[32] S.K. Patil, B.T. Vibhute, Synthesis, characterization, anticancer and DNA photocleavage study of novel quinoline Schiff base and its metal complexes, Arab. J. Chem. 14 (2021) 103285. https://doi.org/10.1016/j.arabjc.2021.103285.

[33] L.Q. Du, T.Y. Zhang, X.M. Huang, Y. Xu, M.X. Tan, Y. Huang, Y. Chen, Q.P. Qin, Synthesis and anticancer mechanisms of zinc(II)-8-hydroxyquinoline complexes with 1,10-phenanthroline ancillary ligands, Dalton Trans. 52 (2023) 4737–4751. https://doi.org/10.1039/d3dt00150d.

[34] W.Y. Shen, C.P. Jia, L.Y. Liao, L.L. Chen, C. Hou, Y.H. Liu, H. Liang, Z.F. Chen, Copper(II) complexes of halogenated quinoline schiff base derivatives enabled cancer therapy through glutathione-assisted chemodynamic therapy and inhibition of autophagy flux, J. Med. Chem. 65 (2022) 5134–5148. https://doi.org/10.1021/acs.jmedchem.2c00133.

[35] A. V. Ermolaev, V.G. Shtyrlin, A.I. Gizatullin, M.A. Zhernakov, N.Y. Serov, K. V. Urazaeva, M.S. Bukharov, E.M. Gilyazetdinov, D.R. Islamov, A.A. Rodionov, I.I.

Mirzayanov, A.R. Garifzyanov, B.K. Kuramshin, Development of comprehensive approaches to characterizing Cu(II) complexes: Structures in solution and solid-state, dynamic behavior, and bioactivity, ChemistrySelect. 8 (2023) 25–29. https://doi.org/10.1002/slct.202303333.

[36] U. Das, P. Paira, Synthesis, characterization, photophysical and electrochemical properties, and biomolecular interaction of 2,2′-biquinoline based phototoxic Ru(II)/Ir(II) complexes, Dalton Trans. 52 (2023) 12608–12617. https://doi.org/10.1039/d3dt01348k.

[37] Z. Hou, A.S. Vanecek, J.J. Tepe, A.L. Odom, Synthesis, structure, properties, and cytotoxicity of a (quinoline)RuCp$^+$ complex, Dalton Trans. 52 (2023) 721–730. https://doi.org/10.1039/D2DT03484K.

[38] T. Pivarcsik, V. Pósa, H. Kovács, N. V. May, G. Spengler, S.P. Pósa, S. Tóth, Z. Nezafat Yazdi, C. Özvegy-Laczka, I. Ugrai, I. Szatmári, G. Szakács, É.A. Enyedy, Metal complexes of a 5-nitro-8-hydroxyquinoline-proline hybrid with enhanced water solubility targeting multidrug resistant cancer cells, Int. J. Mol. Sci. 24 (2023) 593. https://doi.org/10.3390/ijms24010593.

[39] M. Gobec, J. Kljun, I. Sosič, I. Mlinarič-Raščan, M. Uršič, S. Gobec, I. Turel, Structural characterization and biological evaluation of a clioquinol-ruthenium complex with copper-independent antileukaemic activity, Dalton Trans. 43 (2014) 9045–9051. https://doi.org/10.1039/c4dt00463a.

[40] R.P. Paitandi, S. Mukhopadhyay, R.S. Singh, V. Sharma, S.M. Mobin, D.S. Pandey, Anticancer activity of iridium(III) complexes based on a pyrazole-appended quinoline-based BODIPY, Inorg. Chem. 56 (2017) 12232–12247. https://doi.org/10.1021/acs.inorgchem.7b01693.

[41] Q.Y. Yang, Q.Q. Cao, Q.P. Qin, C.X. Deng, H. Liang, Z.F. Chen, Syntheses, crystal structures, and antitumor activities of copper(II) and nickel(II) complexes with 2-((2-(pyridin-2-yl)hydrazono)methyl)quinolin-8-ol, Int. J. Mol. Sci. 19 (2018) 1874. https://doi.org/10.3390/ijms19071874.

[42] T. Thirunavukkarasu, H.A. Sparkes, K. Natarajan, Quinoline based Pd(II) complexes: Synthesis, characterization and evaluation of DNA/protein binding, molecular docking and in vitro anticancer activity, Inorg. Chim. Acta. 482 (2018) 229–239. https://doi.org/10.1016/j.ica.2018.06.003.

[43] F.Y. Wang, K. Bin Huang, H.W. Feng, Z.F. Chen, Y.N. Liu, H. Liang, New Platinum(II) agent induces bimodal death of apoptosis and autophagy against A549 cancer cell, Free Radic Biol Med 129 (2018) 418-429. https://doi.org/10.1016/j.freeradbiomed.2018.09.040.

[44] L. Doan, Modifying superparamagnetic iron oxide nanoparticles as methylene blue adsorbents: A review, ChemEngineering. 7 (2023) 77. https://doi.org/10.3390/chemengineering7050077.

[45] S. Gai, L.He, M. He, X. Zhong, C. Jiang,Y. Qin, M. Jiang, Anticancer activity and mode of action of Cu (II), Zn (II), and, Mn(II) complexes with 5-chloro-2-N-(2-quinolylmethylene)aminophenol, Molecules 28 (2023) 4876. https://doi.org/10.3390/molecules28124876.

[46] D.J.H. De Clercq, D.E. Heppner, C. To, J. Jang, E. Park, C.H. Yun, M. Mushajiang, B.H. Shin, T.W. Gero, D.A. Scott, P.A. Jänne, M.J. Eck, N.S. Gray, Discovery and optimization of dibenzodiazepinones as allosteric mutant-selective EGFR inhibitors, ACS Med. Chem. Lett. 10 (2019) 1549–1553. https://doi.org/10.1021/acsmedchemlett.9b00381.

[47] A. Krstic, A. Pavic, E. Avdovic, Z. Markovic, M. Stevanovic, I. Petrovic, Coumarin-palladium(II) complex acts as a potent and non-toxic anticancer agent against pancreatic carcinoma cells, Molecules 27 (2022) 1–17. https://doi.org/10.3390/molecules27072115.

[48] Q. Wang, Y. Chen, G. Li, Z. Liu, J. Ma, M. Liu, D. Li, J. Han, B. Wang, Synthesis and evaluation of bi-functional 7-hydroxycoumarin platinum(IV) complexes as antitumor agents, Bioorg. Med. Chem. 27 (2019) 2112–2121. https://doi.org/10.1016/j.bmc.2019.04.009.

[49] Ł. Balewski, S. Szulta, A. Jalińska, A. Kornicka, A Mini-Review: Recent advances in coumarin-metal complexes with biological properties, Front. Chem. 9 (2021) 1–18. https://doi.org/10.3389/fchem.2021.781779.

[50] L. Gramni, N. Vukea, A. Chakraborty, W.J. Samson, L.M.K. Dingle, B. Xulu, J.A. de la Mare, A.L. Edkins, I.N. Booysen, Anticancer evaluation of ruthenium(III) complexes with N-donor ligands tethered to coumarin or uracil moieties, Inorganica Chim. Acta. 492 (2019) 98–107. https://doi.org/10.1016/j.ica.2019.04.018.

[51] W. Lu, J. Shi, Y.F. Nie, L. Yang, J. Chen, F. Zhao, S. Yang, L. Xu, X. Chi, Synthesis, crystal structure, antiproliferative activity, DNA binding and density functional theory calculations of 3-(pyridin-2-yl)-8-tert-butylcoumarin and its copper(II) complex, Appl. Organomet. Chem. 34 (2020) 1–11. https://doi.org/10.1002/aoc.5875.

[52] P.D. Mestizo, D.M. Narváez, J.A. Pinzón-Ulloa, D.T. Di Bello, S. Franco-Ulloa, M.A. Macías, H. Groot, G. Pietro Miscione, L. Suescun, J.J. Hurtado, Novel complexes with ONNO tetradentate coumarin Schiff-base donor ligands: X-ray structures, DFT calculations, molecular dynamics and potential anticarcinogenic activity, BioMetals. 34 (2021) 119–140. https://doi.org/10.1007/s10534-020-00268-8.

[53] T. Sarkar, A. Kumar, S. Sahoo, A. Hussain, Mixed-ligand cobalt(III) complexes of a naturally occurring coumarin and phenanthroline bases as mitochondria-targeted dual-purpose photochemotherapeutics, Inorg. Chem. 60 (2021) 6649–6662. https://doi.org/10.1021/acs.inorgchem.1c00444.

[54] K. Schindler, F. Zobi, Anticancer and antibiotic rhenium tri-and dicarbonyl complexes: Current research and future perspectives, Molecules 27 (2022) 539. https://doi.org/10.3390/molecules27020539.

[55] M.S. Capper, H. Packman, M. Rehkämper, Rhenium-based complexes and in vivo testing: A brief history, ChemBioChem. 21 (2020) 2111–2115. https://doi.org/10.1002/cbic.202000117.

[56] A. Sharma S, V. Nee, B. Kar, U. Das, P. Paira, Target-specific mononuclear and binuclear rhenium(I) tricarbonyl complexes as upcoming anticancer drugs, RSC Adv. 12 (2022) 20264–20295. https://doi.org/10.1039/d2ra03434d.

[57] C.C. Konkankit, A.P. King, K.M. Knopf, T.L. Southard, J.J. Wilson, In vivo anticancer activity of a rhenium(I) tricarbonyl complex, ACS Med. Chem. Lett. 10 (2019) 822–827. https://doi.org/10.1021/acsmedchemlett.9b00128.

[58] E.B. Bauer, A.A. Haase, R.M. Reich, D.C. Crans, F.E. Kühn, Organometallic and coordination rhenium compounds and their potential in cancer therapy, Coord. Chem. Rev. 393 (2019) 79–117. https://doi.org/https://doi.org/10.1016/j.ccr.2019.04.014.

[59] A. Bistrović, N. Stipaničev, T. Opačak-Bernardi, M. Jukić, S. Martinez, L. Glavaš-Obrovac, S. Raić-Malić, Synthesis of 4-aryl-1,2,3-triazolyl appended natural coumarin-related compounds with antiproliferative and radical scavenging activities and intracellular ROS production modification, New J. Chem. 41 (2017) 7531–7543. https://doi.org/10.1039/C7NJ01469D.

[60] T.G. Kraljević, A. Harej, M. Sedić, S.K. Pavelić, V. Stepanić, D. Drenjančević, J. Talapko, S. Raić-Malić, Synthesis, in vitro anticancer and antibacterial activities and in silico studies of new 4-substituted 1,2,3-triazole–coumarin hybrids, Eur. J. Med. Chem. 124 (2016) 794–808. https://doi.org/10.1016/j.ejmech.2016.08.062.

[61] A. Meščić Macan, N. Perin, S. Jakopec, M. Mioč, M.R. Stojković, M. Kralj, M. Hranjec, S. Raić-Malić, Synthesis, antiproliferative activity and DNA/RNA-binding properties of mono- and bis-(1,2,3-triazolyl)-appended benzimidazo[1,2-*a*]quinoline derivatives, Eur. J. Med. Chem. 185 (2020) 111845. https://doi.org/10.1016/j.ejmech.2019.111845.

[62] S. Jakopec, L. Gourdon-Grünewaldt, I. Čipor, A. Meščić Macan, B. Perić, I. Piantanida, K. Cariou, G. Gasser, S.I. Kirin, S. Raić-Malić, Synthesis, characterisation and biological evaluation of monometallic Re(I) and heterobimetallic Re(I)/Fe(II) complexes with a 1,2,3-triazolyl pyridine chelating moiety, Dalton Trans. 52 (2023) 9482–9498. https://doi.org/10.1039/d3dt01070h.

[63] S. Maračić, S. Jakopec, M. Piškor, M. Leventić, J. Lapić, S. Djaković, M. Cetina, L. Glavaš-Obrovac, S. Raić-Malić, Mechanochemical synthesis and antiproliferative activity of novel ferrocene quinoline/quinolone hybrids, Appl. Organomet. Chem. 37 (2023) e7124. https://doi.org/10.1002/aoc.7124.

[64] I. Sokol, M. Toma, M. Krnić, A.M. MacAn, D. Drenjančević, S. Liekens, S. Raić-Malić, T.G. Kraljević, Transition metal-catalyzed synthesis of new 3-substituted coumarin derivatives as antibacterial and cytostatic agents, Future Med. Chem. 13 (2021) 1865–1884. https://doi.org/10.4155/fmc-2021-0161.

[65] S. Maračić, J. Lapić, S. Djaković, T. Opačak-Bernardi, L. Glavaš-Obrovac, V. Vrček, S. Raić-Malić, Quinoline and ferrocene conjugates: Synthesis, computational study and biological evaluations, Appl. Organomet. Chem. 33 (2019) 1–17. https://doi.org/10.1002/aoc.4628.

[66] S. Jakopec, L. Hamzic, L. Bočkor, I. Car, B. Perić, S. I. Kirin, M. Sedić, S. Raić-Malić, Coumarin-modified ruthenium complexes: Synthesis, characterization, and antiproliferative activity against human cancer cells, Arch. Pharm. (Weinheim) (2024) e2400271. https://doi.org/10.1002/ardp.202400271.

[67] G.Z. Yang, J.K. Zhu, X.D. Yin, Y.F. Yan, Y.L. Wang, X.F. Shang, Y.Q. Liu, Z.M. Zhao,

J.W. Peng, H. Liu, Design, Synthesis, and antifungal evaluation of novel quinoline derivatives inspired from natural quinine alkaloids, J. Agric. Food Chem. 67 (2019) 11340–11353. https://doi.org/10.1021/acs.jafc.9b04224.

[68] A.F. Borsoi, L.M. Alice, N. Sperotto, A.S. Ramos, B.L. Abbadi, F.S. Macchi Hopf, A. Da Silva Dadda, R.S. Rambo, R.B. Madeira Silva, J.D. Paz, K. Pissinate, M.N. Muniz, C.E. Neves, L. Galina, L.C. González, M.A. Perelló, A. De Matos Czeczot, M. Leyser, S.D. De Oliveira, G. De Araújo Lock, B.V. De Araújo, T.D. Costa, C.V. Bizarro, L.A. Basso, P. Machado, Antitubercular activity of novel 2-(quinoline-4-yloxy)acetamides with improved drug-like properties, ACS Med. Chem. Lett. 13 (2022) 1337–1344. https://doi.org/10.1021/acsmedchemlett.2c00254.

[69] Rigaku Oxford Diffraction CrysAlisPro, CrysAlisPro, (2018).

[70] A.A. Jambol, M.H.S.A. Hamid, A.H. Mirza, M.S. Islam, M.R. Karim, Some novel Schiff bases from pyruvic acid with amines containing N & S donor atoms: synthesis, spectral studies and X-ray crystal structures, Int. J. Org. Chem. 7 (2017) 42–56. https://doi.org/10.4236/ijoc.2017.71005.

[71] G.M. Sheldrick, Crystal structure refinement with SHELXL, Acta Crystallogr. Sect. C Struct. Chem. 71 (2015) 3–8. https://doi.org/10.1107/S2053229614024218.

[72] V. Komreddy, K. Ensz, H. Nguyen, D.P. Rillema, C.E. Moore, Design, synthesis, and photophysical properties of Re(I) tricarbonyl 1,10-phenanthroline complexes, J. Mol. Struct. 1223 (2020) 128739. https://doi.org/10.1016/j.molstruc.2020.128739.

[73] M.R. Boyd, K.D. Paull, Some practical considerations and applications of the National cancer institute in vitro anticancer drug discovery screen, Drug Dev. Res. 34 (1995) 91–109. https://doi.org/10.1002/ddr.430340203.

[74] T. Mosmann, Rapid colorimetric assay for cellular growth and survival: Application to proliferation and cytotoxicity assays, J. Immunol. Methods. 65 (1983) 55–63. https://doi.org/10.1016/0022-1759(83)90303-4.

[75] H.C. Bertrand, S. Clède, R. Guillot, F. Lambert, C. Policar, Luminescence modulations of rhenium tricarbonyl complexes induced by structural variations, Inorg. Chem. 53 (2014) 6204–6223. https://doi.org/10.1021/ic5007007.

[76] W.K.C. Lo, G.S. Huff, J.R. Cubanski, A.D.W. Kennedy, C.J. McAdam, D.A. McMorran, K.C. Gordon, J.D. Crowley, Comparison of inverse and regular 2-pyridyl-1,2,3-triazole “click” complexes: structures, stability, electrochemical, and photophysical properties, Inorg. Chem. 54 (2015) 1572–1587. https://doi.org/10.1021/ic502557w.

[77] D.X. Ngo, W.W. Kramer, B.J. McNicholas, H.B. Gray, B.J. Brennan, Structure, spectroscopy, and electrochemistry of manganese(I) and rhenium(I) quinoline oximes, Inorg. Chem. 58 (2019) 737–746. https://doi.org/10.1021/acs.inorgchem.8b02862.

[78] T.T. Zhang, J.F. Jia, Y. Ren, H.S. Wu, Ligand effects on structures and spectroscopic properties of pyridine-2-aldoxime complexes of $Re(CO)_3^+$: DFT/TDDFT theoretical studies, J. Phys. Chem. A. 115 (2011) 3174–3181. https://doi.org/10.1021/jp200872b.

[79] X. Jia, K. Cui, J.L. Alvarez-Hernandez, C.L. Donley, A. Gang, S. Hammes-Schiffer, N.

Hazari, S. Jeon, J.M. Mayer, H.S. Nedzbala, B. Shang, E.A. Stach, E. Stewart-Jones, H. Wang, A. Williams, Synthesis and surface attachment of molecular Re(I) hydride species with silatrane functionalized bipyridyl ligands, Organometallics. 42 (2023) 2238–2250. https://doi.org/10.1021/acs.organomet.3c00235.

[80] L.E. Enslin, K. Purkait, M.D. Pozza, B. Saubamea, P. Mesdom, H.G. Visser, G. Gasser, M. Schutte-Smith, Rhenium(I) tricarbonyl complexes of 1,10-phenanthroline derivatives with unexpectedly high cytotoxicity, Inorg. Chem. 62 (2023) 12237–12251. https://doi.org/10.1021/acs.inorgchem.3c00730.

[81] K. Łyczko, A. Pogorzelska, U. Częścik, M. Koronkiewicz, J.E. Rode, E. Bednarek, R. Kawęcki, K. Węgrzyńska, A. Baraniak, M. Milczarek, J.C. Dobrowolski, Tricarbonyl rhenium(I) complexes with 8-hydroxyquinolines: structural, chemical, antibacterial, and anticancer characteristics, RSC Adv. 14 (2024) 18080–18092. https://doi.org/10.1039/d4ra03141e.

[82] A.M. Almehdi, S.S.M. Soliman, A.N.A. El-Shorbagi, A.D. Westwell, R. Hamdy, Design, synthesis, and potent anticancer activity of novel indole-based Bcl-2 inhibitors, Int. J. Mol. Sci. 24 (2023) 14656. https://doi.org/10.3390/ijms241914656.

[83] P. V. Simpson, I. Casari, S. Paternoster, B.W. Skelton, M. Falasca, M. Massi, Defining the anti-cancer activity of tricarbonyl rhenium complexes: induction of g2/m cell cycle arrest and blockade of aurora-A kinase phosphorylation, Chem. A Eur. J. 23 (2017) 6518–6521. https://doi.org/10.1002/chem.201701208.

[84] T. Dettori, G. Sanna, A. Cocco, G. Serreli, M. Deiana, V. Palmas, V. Onnis, L. Pilia, N. Melis, D. Moi, P. Caria, F. Secci, Synthesis and antiproliferative effect of halogenated coumarin derivatives, Molecules 27 (2022) 1–14. https://doi.org/10.3390/molecules27248897.

[85] L. Krstulović, K. Mišković Špoljarić, V. Rastija, N. Filipović, M. Bajić, L. Glavaš-Obrovac, Novel 1,2,3-triazole-containing quinoline-benzimidazole hybrids: Synthesis, antiproliferative activity, in silico ADME predictions, and docking, Molecules 28 (2023) 6950. https://doi.org/10.3390/molecules28196950.

[86] L. Krstulović, I. Stolić, M. Jukić, T. Opačak-Bernardi, K. Starčević, M. Bajić, L. Glavaš-Obrovac, New quinoline-arylamidine hybrids: Synthesis, DNA/RNA binding and antitumor activity, Eur. J. Med. Chem. 137 (2017) 196–210. https://doi.org/10.1016/j.ejmech.2017.05.054.

[87] S. Duanghathaipornsuk, E.J. Farrell, A.C. Alba-Rubio, P. Zelenay, D.S. Kim, Detection technologies for reactive oxygen species: Fluorescence and electrochemical methods and their applications, Biosens. 11 (2021) 30. https://doi.org/10.3390/BIOS11020030.

[88] X. Li, Y. Wang, M. Li, H. Wang, X. Dong, Metal complexes or chelators with ROS regulation capacity: Promising candidates for cancer treatment, Molecules 27 (2022) 1–15. https://doi.org/10.3390/molecules27010148.

[89] M.A. Shah, H.A. Rogoff, Implications of reactive oxygen species on cancer formation and its treatment, Semin. Oncol. 48 (2021) 238–245. https://doi.org/10.1053/j.seminoncol.2021.05.002.

[90] P. Mucha, P. Hikisz, K. Gwoździński, U. Krajewska, A. Leniart, E. Budzisz, Cytotoxic effect, generation of reactive oxygen/nitrogen species and electrochemical properties of Cu(II) complexes in comparison to half-sandwich complexes of Ru(II) with aminochromone derivatives, RSC Adv. 9 (2019) 31943–31952. https://doi.org/10.1039/c9ra05971g.

[91] L.T. Todorov, I.P. Kostova, Coumarin-transition metal complexes with biological activity: current trends and perspectives, Front. Chem. 12 (2024) 1–15. https://doi.org/10.3389/fchem.2024.1342772.

[92] M. Sharma, V.K. Vyas, S. Bhatt, M.D. Ghate, Therapeutic potential of 4-substituted coumarins: A conspectus, Eur. J. Med. Chem. Reports. 6 (2022) 100086. https://doi.org/10.1016/j.ejmcr.2022.100086.

[93] C. Iacobini, M. Vitale, C. Pesce, G. Pugliese, S. Menini, Diabetic complications and oxidative stress: A 20-year voyage back in time and back to the future, Antioxidants 10 (2021) 727. https://doi.org/10.3390/antiox10050727.

[94] C. Fernandes, A.J.C. Videira, C.D. Veloso, S. Benfeito, P. Soares, J.D. Martins, B. Gonçalves, J.F.S. Duarte, A.M.S. Santos, P.J. Oliveira, F. Borges, J. Teixeira, F.S.G. Silva, Cytotoxicity and mitochondrial effects of phenolic and quinone-based mitochondria-targeted and untargeted antioxidants on human neuronal and hepatic cell lines: A comparative analysis, Biomolecules 11 (2021) 1605. https://doi.org/10.3390/biom11111605.

[95] T. Satoh, Y. Enokido, H. Aoshima, Y. Uchiyama, H. Hatanaka, Changes in mitochondrial membrane potential during oxidative stress- induced apoptosis in PC12 cells, J. Neurosci. Res. 50 (1997) 413–420. https://doi.org/10.1002/(SICI)1097-4547(19971101)50:3%3C413::AID-JNR7%3E3.0.CO;2-L.